1-1-1999

Theoretical study of MBE growth of indium gallium arsenide semiconductor compound on gallium arsenide substrate

Golshan Colayni
University of Nevada, Las Vegas

INFORMATION TO USERS

This manuscript has been reproduced from the microfilm master. UMI films the text directly from the original or copy submitted. Thus, some thesis and dissertation copies are in typewriter face, while others may be from any type of computer printer.

The quality of this reproduction is dependent upon the quality of the copy submitted. Broken or indistinct print, colored or poor quality illustrations and photographs, print bleedthrough, substandard margins, and improper alignment can adversely affect reproduction.

In the unlikely event that the author did not send UMI a complete manuscript and there are missing pages, these will be noted. Also, if unauthorized copyright material had to be removed, a note will indicate the deletion.

Oversize materials (e.g., maps, drawings, charts) are reproduced by sectioning the original, beginning at the upper left-hand corner and continuing from left to right in equal sections with small overlaps.

Photographs included in the original manuscript have been reproduced xerographically in this copy. Higher quality 6" x 9" black and white photographic prints are available for any photographs or illustrations appearing in this copy for an additional charge. Contact UMI directly to order.

Bell & Howell Information and Learning
300 North Zeeb Road, Ann Arbor, MI 48106-1346 USA

UMI®
800-521-0600

THEORETICAL STUDY OF MBE GROWTH OF InGaAs SEMICONDUCTOR COMPOUND ON GaAs SUBSTRATE

by

Golshan Colayni

Bachelor of Science
Sharif University, Tehran, Iran
1991

Master of Science
Azad University, Tehran, Iran
1993

A thesis submitted in partial fulfillment
of the requirements for the

Master of Science
Department of Computer and Electrical Engineering
Howard R. Hughes College of Engineering

Graduate College
University of Nevada, Las Vegas
December 1999

UNLV
UNLV

Thesis Approval
The Graduate College
University of Nevada, Las Vegas

September 16, 1999

The Thesis prepared by

Golshan Colayni

Entitled

Theoretical Study of Molecular Beam Epitaxy growth of InGaAs compound Semiconductor on Gallium Arsenid Substrate

is approved in partial fulfillment of the requirements for the degree of

Master of Science in Electrical Engineering

Examination Committee Chair

Dean of the Graduate College

Examination Committee Member

Examination Committee Member

Graduate College Faculty Representative

ABSTRACT

Theoretical Study of MBE Growth of InGaAs Semiconductor Compound on GaAs Substrate

by

Golshan Colayni

Dr. Rama Venkat, Examination Committee Chair
Professor of Electrical Engineering
University of Nevada, Las Vegas

The theoretical study of Molecular Beam Epitaxy allows us to model and construct an experiment with the same conditions. Growth modeling investigates compound semiconductor characteristics during the MBE growth which can achieve the best results to control the quality of growth. Growth modeling also is less expensive and faster than experiments. The wide variation in the band-gap and lattice constants between $InAs$ and $GaAs$ is a subject for a variety of optical and electronic device applications involving $InGaAs/GaAs$ systems. In this material system, the perfection is intrinsically controlled by the surface segregation of In due to its larger atomic size compared to Ga. In this work, a rate equation model is developed including several surface processes such as segregation from the crystalline layer to a surface riding In segregated layer and incorporation from the segregated In layer to crystalline layer and gallium desorption to surface layer. The rate of the processes are assumed Arrhenius type with concentration dependent activation energies. The simulated In incorporation coefficient versus substrate temperature is in excellent agreement with the experimental data [1] for various As overpressure. For a constant As overpressure, In incorporation decreases with increasing temperature. For a constant temperature,

In incorporation increases with increasing *As* overpressure. The *In* desorption versus time results from experiments and our simulation match very well. The desorption process has two components, one arising from the physisorbed layer of *In* and the other from the surface of the crystal. The activation energy for these processes for an isolated adatom are 0.18 eV and 2.6 eV, respectively. These observations are explained based on the interplay of competing surface processes such as segregation and incorporation.

TABLE OF CONTENTS

LIST OF FIGURES

ACKNOWLEDGMENTS

I would like to show my appreciation to my advisor Dr. Venkat for his priceless guidance and advice. I would also like to thank Dr. Shahram Latifi, Dr. Rahim Khoie and Dr. Changfeng Chen, for their precious support by accepting to be on my graduate committee. I would like to acknowledge the support of the Air Force Office of Scientific Research under Defense Experimental Program to Stimulate Competitive Research (DEPSCoR), grant number F49620-96-0275.

I like to thank all the faculty and staff of the Department of Electrical Engineering, University of Nevada, Las Vegas for their inestimable help. I am also grateful my family for their patience throughout the course of this study.

CHAPTER 1

INTRODUCTION

1.1 Objective of the Thesis

Today, the increasing demand for advance semiconductor device technology has attracted researchers to study a wide variety of issues in semiconductor fabrication. Molecular beam epitaxy (MBE) is one of the most interesting growth techniques to produce fast opto-electronic devices with unique optical and electronic properties. Molecular beam epitaxy is an epitaxial process that employs evaporated material on heated substrate under ultra vacuum of 10^{-8} to 10^{-10} torr. MBE technique has a number of advantages over the traditional techniques such as chemical vapor deposition (CVD). The main advantage is low-temperature processing. Low-temperature processing minimizes out-diffusion and out-doping. Another advantage is the precise control of doping, and thickness control to atomic dimensions that MBE technique allows. MBE technique also allows $in-situ$ monitoring of growth control during the growth processes through several analytical tools. Reflective high-energy electron diffraction (RHEED) is one of the experimental tools to monitor cation and anion incorporation rates, alloy composition, and oxide desorption. It is also an important tool to measure growth rate and thickness [21]. The $in-situ$ reflection mass spectroscopy (REMS) is one of the analytical tools in MBE growth for measuring of native oxide desorption, sticking coefficients of group III, desorption rates, incorporation rates and fluxes [8]. Effective segregation during $InGaAs/GaAs$ growth can be observed by using both $in-situ$ RHEED, $ex-situ$ secondary ion mass spectrometry

(SIMS) and photoluminescence (PL)[8].

The *InGaAs/GaAs* is one of compound semiconductors which has a variety application in solid state microwave, optoelectronic technologies, quantum well devices, and semiconductor lasers. It has been reported that device performance can be improved if the base of the transistor is fabricated from *InGaAs* [65]. Electron transport in *InGaAs* has some very remarkable features for microwave applications. The great interest in this system for device application is due to the electronic and optical properties of band gap and lattice constant differences between *GaAs* and *InAs* [1]. Particularly, the *InGaAs/GaAs* heteroepitaxial system can be used in monolithic integration of optoelectronic devices for near infrared and for visible light regions [21].

The growth dynamics of the *InGaAs/GaAs* system have been investigated for understanding of important surface processes. Investigation of the molecular beam epitaxy (MBE) dynamic processes is for controlling growth processes and improving reliability and productivity. Several studies [1-19] have shown that the dynamic of processes during the growth of *InGaAs* are complex, particularly at temperatures where indium desorption, segregation, and incorporation are all important.

In spite of the interest and experimental work on the growth processes and device applications, the understanding of the growth processes for the reliable control of the growth is limited. In this thesis, a rate equation is employed to model the *InGaAs* alloy semiconductor MBE growth. *In* incorporation coefficient versus substrate temperature and *In* and *Ga* desorption versus growth time are investigated and compared with experimental results using numerical simulation of the model to validate the model.

1.2 Organization of the Thesis

The thesis is organized in to five chapters. The overview of MBE growth, properties and application of *InGaAs* devices, experimental dynamic studies of *InGaAs* MBE growth and theoretical models employed for growth studies relevant to this thesis are discussed in chapter 2. The physical and mathematical basis of the theoretical model along with all equations related to the model are described in chapter 3. Chapter 4 is devoted to a discussion of fitting procedure to obtain the theoretical model parameters, results and the limitation of the model. Finally the conclusions and recommendations regarded to this study are given in Chapter 5.

CHAPTER 2

LITERATURE SURVEY OVERVIEW

2.1 Molecular Beam Epitaxy

The word "epitaxy" is originally from the Greek words "epi" meaning "upon", and " taxis" meaning "to arrange". Thus, epitaxy means the ability to add and to arrange atoms upon a single crystalline surface of a substrate. Epitaxial growth is a growing process of one material on a single crystal substrate of the same material (homoepitaxy) or of a different material and chemical composition (heteroepitaxy). Epitaxial films of semiconductors can be grown from vapor phase epitaxy (VPE) using chemical vapor growth epitaxy (CVE) or physical vapor growth such as molecular beam epitaxy (MBE), and liquid phase epitaxy (LPE). Each technique has its own advantages and disadvantages. MBE technique is one of the sophisticated techniques which requires high vacuum equipment that can produce vacuum in the order of 10^{-8} torr. This technique has the capability to allow abrupt changes in doping or in composition, to control precisely of very thin films monolayers, to grow high quality multilayer structures in relatively low temperatures and minimizing out-diffusion. Due to precise control of the beam fluxes, highly order crystalline films of one or more material layers can be deposited.

In MBE technique, the molecular beams are generated under UHV conditions normally from Knudsen-effusion-cells containing the constituent elements whose temperatures are accurately controlled to achieve a good flux stability. Computer controlled temperatures of the substrate and each of the sources and the operation of shutters,

dictate the desired chemical composition and the doping of the epitaxial films. The molecules of different species of beams have negligible collisions or interactions before reaching the surface of the substrate as their mean free paths are very long. Epitaxial growth occurring on the substrate surface involves a series of surface processes like adsorption of the atoms on the substrate surface, surface migration of the adsorbed atoms, incorporation of the atoms into the crystal lattice and thermal desorption of the species. The crystal surface has crystal lattice sites created by the surface dangling bonds and are characterized by their individual chemical activity.

The growing surface is accessible for observation atom using powerful real-time surface-science diagnostics. The ultra-high vacuum allows monitoring of the growth with $in-situ$ tools like reflection high-energy electron diffraction (RHEED). RHEED is routinely used to monitor the crystal structure and microstructure of growing surfaces. Reflection mass spectrometry (REMS) and modulated beam mass spectrometry (MBMS) are used to monitor the chemistry of growing surfaces, and reflectance difference spectroscopy (RDS) is used to monitor the composition and optical properties of the growing surfaces. Surface segregation in the growth of alloy materials can be studied via surface sensitive techniques such as auger electron spectroscopy (AES), x-ray photoemission spectroscopy (XPS) and combination of secondary ion mass spectroscopy(SIMS) and photoluminescence (PL)[9]. Temperature-programmed desorption (TPD) [6] is also employed to investigate the tendency of indium to segregate at the surface of $InGaAs$ films during molecular beam epitaxy. TPD analysis is used for quantitive assessment of surface populations and binding energies of adsorbed species present on solid surfaces. The TPD analysis of the surface indium population can be carried out as a function of $InGaAs$ thickness, $GaAs$ cap thickness, growth temperature and incident arsenic dimer flux.

In a nutshell, the device engineer can control and produce the state of the surface

including composition, crystal structure and smoothness and subsequently, the quality of the material very precisely. The surface scientist can study, directly, the real-time evolution of surface structure, micro structure and composition.

2.2 Difference Between VI Elemental and III-V Compound Semiconductors

Semiconductors such as Si, Ge, C, etc have a diamond structure with the same atom on both sublattices. If the atoms are different in the two sublattices, the structure is called zinc blende structures. Semiconductors such as $GaAs, AlAs, CdS$ fall in to this category. Some semiconductors crystallize in the "wurtzite" structure. Wurtzite is similar to the zinc blende structure. Both structures are fourfold coordinated, except that the former has a hexagonal close packed (hcp) Bravis lattice rather than a face centered cubic (fcc). Semiconductors such as $InAs, ZnO, GaN$ have a wurtzite structure.

Semiconductors such as $GaAs$, InP and $InGaAs$ have their bottom of the conduction band and top of the valance band at the same K (momentum vector) location in the energy (E) versus momentum vector (K) plot. Such materials are optically active and are called direct band gap semiconductors. Si, Ge are indirect band gap materials and have very weak interactions with light and can not be used for efficient optical devices.

One of the other advantages, of the III-V compound semiconductors is the high mobility of these materials compared to elemental semiconductors such as Si, Ge, resulting in devices with reduced parasitics and improved frequency response. Room temperature mobilities in high quality $GaAs$ samples are 8500 $cm^2V^{-1}s^{-1}$ compared to only 1500 $cm^2V^{-1}s^{-1}$ for Si. One of the semiconductors which is important for high speed devices is $In_{0.53}Ga_{0.47}As$. This material has a very high room temperature mobility of about 11000 $cm^2V^{-1}s^{-1}$. At low temperature, the mobility is dominated

by alloy scattering effects, and is less than, the mobility in pure *GaAs* low field [69].

The greatest impact of compound semiconductors has been in areas where their unique properties allow functions that can not be performed by silicon. These include transferred electron devices, light-emitting diodes, lasers and infrared photodetectors. Of the many compound semiconductors currently under investigation, gallium arsenide and related compounds are the most technologically advanced.

2.3 Application of InGaAs Compound Semiconductor Devices

The importance of ternary compound semiconductor devices and their application form the foundation of solid-state microwave and optoelectronic technologies used in many modern communication systems. It has been reported that device performance can be improved if the base of the transistor is fabricated from *InGaAs* for following reasons:

- The reduction of the band-gap in *InGaAs* compared with *GaAs* gives a greater emitter-base valance band offset. This helps to ensure that holes are not reverse injected into the emitter.

- The higher electron mobility in the base allows a shorter base transit time and a consequent improvement in device speed.

- The hole mobility is dependent on the direction of the strain, being higher in growth plane with consequent lower base sheet resistance, and lower perpendicular to the growth plane and hence limiting the movement of the holes in that direction.

- The lower growth temperature for *InGaAs* allows more p-type dopant to be incorporated. High doping levels can be achieved, reducing further the sheet resistance.

- There is the possibility of grading the *InGaAs* alloy composition allowing the electrons to be swept out of the base by a high electric field in the conduction band [65].

InGaAs is an excellent material for long haul communications (at 1.55 micrometer). One of the application of *InGaAs* devices is in optical communication system as a p-i-n photo detectors. They provide switching circuitry in optical communication system which use optical fiber instead of metallic cable. Another possible application of compound semiconductor is in semiconductor lasers using quantum wells and quantum dots. Quantum dot (QD) as an active region in a semiconductor injection laser enhances ultra low threshold current density and provides high thermal stability in the semiconductor lasers.

2.4 Incorporation of In in InGaAs MBE Growth

Indium incorporation coefficient as a function of substrate temperature [1,5,9,10,15] and growth time [2,11] have been studied experimentally for various V/III ratios, *In* compositions and *As* molecular specious, i.e. As_2 and As_4. Indium incorporation is enhanced by using high V/III ratio and arsenic dimer, As_2. It is observed that there is *In* enrichment at the surface of the interface in heterointerfaces involving *InGaAs*.

Woodbridge *et al* [10] studied indium incorporation in *InGaAs* grown by MBE, at a growth rate of 1 monolayer/second (ML/s), temperature of 550°C and various *As* overpressures. They found that the free *In* surface population can be suppressed by increasing the *As* flux. The growth of *InGaAs/GaAs* quantum well structures at temperatures above about 550°C may therefore be improved using high V/III ratios or by the use of a growth interruption at the *InGaAs/GaAs* interface.

2.5 Indium Segregation Studies

Muraki *et al* [9] investigated the surface segregation of *In* atoms during MBE growth and its influence on the energy levels in *InGaAs/GaAs* quantum wells (QWs), by combining secondary-ion mass spectroscopy (SIMS) and photoluminescence (PL). The growth rate was about 0.7 μm/h for *InGaAs*. They developed a model for interpreting their experimental results. In their model, the segregation probability R is calculated from the segregation length (λ) obtained from secondary ion mass spectroscopy (SIMS) measurement and using the relation $R = exp(-d/\lambda)$, where d is half the lattice constant of *GaAs* (2.83Å). They observed that when growth temperature is raised from 370°C to 520°C, the segregation length increases from 0.8 to 2.9 nm. They showed that the indium surface segregation length is highly dependent on growth temperature for low V/III flux ratios of 4 and 12.

Kao *et al* [8] studied the segregation ratio R under various deposition conditions in real-time. Kao performed experiments similar to those of Muraki *et al* [9]. *In-situ* reflection mass spectroscopy (REMS) was used for real-time monitoring of surface composition during epitaxial layer growth to improve control of *InGaAs* compositions. They found that throughout the temperature range 470-560°C, the REMS signal dependence yields an activation energy (4.08 eV) which agrees well with that of Evans *et al* [5]. The high values of R (0.7-0.8) were observed under normal device layer growth produces a surfaces layer with high *In* content (i.e., *InAs*). They suggested a model for segregation process where the segregation ratio R is defined as the fraction of *In* atoms on the top layer which segregate to the next layer. Only $(1 - R)$ of the total surface *In* incorporates into the growing film. The *In* composition in the n^{th} monolayer is then:

$$x_n = x_0(1 - R^n), (0 < n < N : \text{in the InGaAs layer}) \qquad (2.1)$$

$$x_n = x_0(1 - R^n)R^{n-N}, (n > N : \text{in the GaAs overlayer}) \quad (2.2)$$

where x_0 and N are the nominal In mole fraction and the QW width in monolayer, respectively.

Woodbridge *et al* [10] found that indium segregates to the surface during growth above 550°C and a constant surface concentration results at low indium flux. They found that up to two mono-layers of indium may have segregated onto the surface during the growth of 200 Åof $In_{0.25}Ga_{0.75}As$ at 560°C. They also observed the indium segregation at higher substrate temperature under the effects of indium flux and for V/III flux ratios of 20 and 30.

Hazay *et al* [17] studied the segregation to the surface of various third-column atoms in ternary arsenide ($GaAlAs$, $InAlAs$, $InGaAs$) grown by molecular beam epitaxy. The surface segregation of third-column atoms used ternary alloys ($Ga_{0.7}Al_{0.3}As$, $In_{0.52}Al_{0.48}As$, $In_{0.53}Ga_{0.47}As$, $In_{0.2}Ga_{0.8}As$) was studied by *in-situ* auger electron spectroscopy (AES) and x-ray photo-emission spectroscopy (XPS). The peak intensities due to the different alloys were considered. Hazay *et al* suggested that an elementary model involving an exponential law with absorption length L provides an excellent match with experimental data. The reduced segregation rate, R, relevant to elements A and B in the alloy $A_xB_{1-x}As$ was found using the follow equations:

$$R_A = x_b + (x_s - x_b)(1 - exp(-\frac{a^*}{L_A})) \quad (2.3)$$

and

$$R_B = 1 - x_b + (x_b - x_s)(1 - exp(-\frac{a^*}{L_B})) \quad (2.4)$$

where a^* is half the lattice constant and x_s and x_b are, the surface and bulk compositions of the A element, respectively. It has been suggested that segregation found at the interfaces could be explained as the difference between 'normal' and 'inverted' interfaces of $InGaAs/GaAs$ system. The tendency of third-column atoms to sur-

face segregation in ternary alloys is summarized by the relation $In > Ga > Al$ as in heterostructure between binary arsenide. The relation shows that indium atoms have the highest tendency to surface segregation. Hazay *et al* showed that during the growth of $InGaAs$ on $GaAs$ by MBE, the indium atoms segregate at a ratio of more than 0.8 under the conventional growth conditions for $InGaAs$. The transition from two-dimensional to three-dimensional growth occurs when the amount of indium reaches to about 1.7 monolayers, with indium composition greater than 0.25.

Kaspi *et al* [7] suggested the use of low substrate temperature and higher V/III ratios as a means of reducing indium surface segregation to improve both normal and inverted interfaces. They found that the surface segregation of indium atoms during MBE of $InGaAs$ layers highly influences the composition in the vicinity of both the normal and the inverted $Ga(Al)As/InGaAs$ interface. They observed that the intended alloy composition in $In_{0.22}Ga_{0.78}As$ is not reached to the actual composition unless it grows until nearly 35Åfrom the $InGaAs$ on $GaAs$ interface for growth temperature 500°C. The compositionally graded region in $InGaAs$ can be eliminated by pre-adsorbing a fixed amount of In onto the $GaAs$ surface to match the surface segregated layer during steady state, before depositing the $InGaAs$ layer. The amount of indium in the floating layer at steady state is observed to more than double from 0.63 monolayer (ML) at 425°C to 1.3 ML at 520°C.

2.6 Indium Desorption

The desorption of group III elements during MBE of III-V semiconductors is of great importance in the control of the thickness and the composition of structures grown [11]. There are two main techniques used in the study of this phenomenon. One way is to observe the temperature dependence of the growth rate and infer the desorption rate [2]. The other is to measure the desorption flux directly by using

modulated beam mass spectroscopy (MBMS) [5,8]. Measurement of the growth rate can be achieved *in-situ* by the reflection high energy electron diffraction (RHEED) intensity oscillation technique or *ex-situ* by layer thickness measurements. One of the distinguishable indium desorption dependences is on the substrate temperature during the growth. This study can be possible by using MBMS [5].

Zhang *et al* [3] investigated *Ga* and *In* desorption in the *InGaAs* and *InAs* layers grown via MBE at relatively high substrate temperatures. For *Ga* desorption studies, *InGaAs* and *InAs* were grown for 10 min at substrate temperatures range of 560°C to 630°C. Indium and gallium molecular beam fluxes were given including As_2 and As_4 were measured using RHEED intensity oscillation and maintained constant. The logarithmic desorption rate of *Ga* from *GaAs* surfaces was plotted against inverse substrate temperature. Two distinct temperature dependences for indium desorption from *InAs* were reported. One is shown to be independent of surface indium adatom population, the other is shown to be dependent on indium adatom population. The two rate limiting processes operate at two different temperature regions and are independent of one another. It is found that there is a small difference in the desorption rate between the two cases Langmuir evaporation and growing conditions. The activation energy for desorption is approximately 4.0 eV[3].

Mozume *et al* [19] studied the indium desorption during the molecular beam epitaxy of *InGaAs/GaAs* growth using RHEED intensity oscillations. The *InAs* mole-fraction was varied from 0.07 to 0.25. *Ga*, *In* and *As* fluxes were monitored by the ion gauge at the substrate position. The V/III flux ratios were varied from 8 to 20. The growth rate was about 0.5 μm/h for *GaAs*. The flux evaporating from the surface was completed by the Hertz-Knudsen-Langmuir equation:

$$J_{In} = 3.51 \times 10^{22} \times (\frac{M}{T})^{\frac{1}{2}} \times P_{torr}(cm^{-2}.s^{-1}) \qquad (2.5)$$

where M is the atomic mass in grams, and P_{torr} is the partial pressure of the evaporating species at T°K. The time for In evaporation, t, from the $In_xGa_{1-x}As$ surface is determined:

$$t = \frac{3.1 \times 10^{14} X}{J_{In}(s^{-1})} \tag{2.6}$$

where X is the indium composition and J_{In} is the indium flux. The indium desorption activation energy obtained from the temperature dependence of $InAs$ growth rate agree well with the enthalpy of $InAs$ decomposition. The RHEED pattern transition time, t_1, for switching from $InGaAs$ to $GaAs$ reconstructions during heteroeptaxial growth of $GaAs$ on $InGaAs$ was found to be independent of $InGaAs$ layer thickness.

Incorporation/desorption rate variation at heterointerfaces in III-V molecular beam epitaxy were studied by Evans *et al* [2,5]. Three heterointerfaces, $AlGaAs$ on $GaAs$, $InGaAs$ on $GaAs$ and $SbGaAs$ on $GaAs$, were investigated. The V/III flux ratios were varied from 8 to 20. The growth rate was about 0.5 μm/h for $GaAs$. A mass spectrometer was used in the experimental method to monitor the desorption rate of partially incorporation species such as In, Al and Sb. The incorporation coefficient α_M of species M is defined by:

$$\alpha_M = 1 - \frac{F_d(M)}{F_i(M)} \tag{2.7}$$

where $F_d(M)$ and $F_i(M)$ are M's desorb and incident fluxes, respectively. The $In_yGa_{1-y}As/GaAs$ system with y=0.15 was studied for substrate temperature between 547 and 637°C. Constant incident fluxes were used (1 monolayer (ML)=2.83Åfor $GaAs$): F_i(In)=0.09 ML/s, F_i(Ga)=0.5 ML/s. The arsenic tetrameric beam flux pressure was 1.38 × 10 $^{-5}$torr. It was observed that incorporation rates vary with time during the growth and it significantly influences the compositional profiles and layer thickness. The indium desorption flux versus time shows that the time required to

reach steady state is about 8 second, or 4 ML growth. As long as indium desorption flux is not varied in a step-like manner and indium desorption is less than expected, the indium composition is not constant during the growth. The variation of the In composition, y's values with position from the $InGaAs/GaAs$ for different substrate temperatures were investigated. The relation between In incorporation coefficient, α_{In}, and y for $In_yGa_{1-y}As$ was suggested to be:

$$y^{-1} = 1 + \frac{F_i(Ga)}{\alpha_{In}F_i(In)} \tag{2.8}$$

The value of $F_d(In)$ for steady state "bulk" $InGaAs$ growth is found to vary with calculated y value, i.e. $F_d(In) = K_d \times y$, K_d is a first order In desorption rate constant. The variation of K_d with temperature is expected to be Arrhenius, i.e.

$$K_d = \nu \times exp(-\frac{E_a}{kT}) \tag{2.9}$$

where ν is a frequency factor and E_a is the activation energy associated with In desorption. An Arrhenius plot of $F_d(In)/y$ gives a value of E_a=3.4 eV[2].

2.7 Strain

There have been several experimental studies reported in the literature to study the effect strain layer on the electrical and optical quality of compound semiconductors [22,23,24,25,26]. $InGaAs$ strained layers on $GaAs$ show useful characteristics, e.g. higher carrier mobility and the splitting of heavy and light holes in the valance band. It has been shown that the $InGaAs$ grown in the substrate temperature range 400-420°C has a mobility more than $6200cm^2V^{-1}s^{-1}$. In this study, highly strained layers grew without misfit dislocations for the In composition range of 0.3 to 0.4. To achieve 2-dimensional electron gas and electron mobility, $In_xGa_{1-x}As$ layers must be grown 6 to 10 nm thick. Misfit dislocation [23] occurrence during growth has been studied by RHEED of $In_xGa_{1-x}As$ on gallium arsenide substrate where indium

composition is x=0.3,0.38 and 0.5. For highly strained layers, it was observed that $GaAs$ must be preserved carefully at 590°C before $InGaAs$ growth. It was observed that the surface energy has a greater effect than the details of dislocation for very thin films. The results are compared with various models of dislocation nucleation and good agreement is found for heterogeneous misfit accommodation by 60 degree dislocations.

Coman *et al* [24] found that in order to reduce the strain in lattice-mismatched during epitaxial growth, one must use thin compliant growth substrates. They also observed that strain can be used to modify molecular beam epitaxy growth kinetics, such as cation desorption and migration. They introduced a new method for producing laterally confined structures which is extremely flexible and can be applied to any material system. Such a method, called strain-modulated epitaxy, utilizes thin, compliant substrates which are patterned on the bottom, bonded surface. The strain produced during growth will be partitioned between the substrate and the lattice-mismatched epitaxial layer according to :

$$\epsilon_f = \frac{h_s}{h_f + h_s}\epsilon_0 \tag{2.10}$$

where ϵ_f is the new strain film, ϵ_0 is the total strain of the system, h_s is the thickness of the substrate, and h_f is the thickness of the grown film.

2.8 RHEED

Reflection high-energy electron diffraction (RHEED) is an integral part of the molecular beam epitaxy chamber to study the initial static semiconductor surface geometries (e.g. surface smoothness, disorder, steps etc.) and stoichiometric phases (e.g. changes of surface reconstruction pattern with respect to substrate temperature). In RHEED, a high energy beam of electrons in the range of 5-40 kV is directed

towards the surface at a grazing angle of about 1° to 3°. This is ideal for MBE where the molecular beams impinge on the surface at near-normal incidence.

Fujita *et al* [27] studied grown $In_xGa_{1-x}As$ layers with various alloy compositions ($0 \leq x \leq 1$) on $GaAs$ substrates. The grown layers and heterointerfaces were characterized by RHEED and X-ray diffraction. The RHEED patterns indicated that the crystal nucleation is two-dimensional throughout the epitaxial growth for $0 \leq x \leq 0.4$, but for $0.5 \leq x \leq 1$, it is three-dimensional at the early stage of the growth followed by two-dimensional growth. All the experimental results consistently showed that the crystalline quality degrades with the increase of x from 0 to about 0.5, but beyond 0.5, it tends to become rather improved with x.

2.9 Comparison of Growth Modeling Techniques

One aim of the numerical simulation is to compare the results with experimental results to validate the physical model. Detailed information calculated by simulation can be achieved faster with less expense. Another feature of the calculation by simulation is to study phenomena which is not amenable to analytical theories. There are several theoretical tools available to study the growth process MBE and metal organic chemical vapor deposition (MOCVD) such as Monte Carlo simulations(MC), molecular dynamics simulation (MD), stochastic models, and rate equation models. The theoretical studies of MBE must be able to probe the surface growth kinetics to predict the macroscopic growth rate as a function of substrate temperature, composition surface and interface roughness, and the partial pressure of the reactants.

The term Monte Carlo refers to the random simulation by calculating the probability distribution of a physical event or series of events based on the expression for the rates. Monte Carlo simulations are based on the rigid lattice of finite size [59,60]. The surface kenitic processes, typically considered in the MC simulation, are

incorporation, surface migration and reevaporation. The rate, K, corresponding to individual processes at the (local) temperatures, T, are usually taken to be of the Arrhenius form, given by:

$$K(T) = K_0 exp(-E/k_B T)$$

where K_0 represents an attempt rate for the process, E is the kinetic energy barrier for the process, k_B is the Boltzmann's constant, and T is the temperature [60]. MC simulation provides macroscopic growth in formation such as growth rate, surface and interface and roughness compositional guiding. It allows RHEED simulation based on kinematic theory of electron diffraction.

Molecular Dynamics (MD) is growth simulation method based on actual atomic dynamics. In this model, no rigid lattice is assumed unlike the MC simulation. In this model, particle experiences and reacts to the potential of the rest of the particles which are held fixed in their position. The potential is usually obtained from a definite physical model. In order to follow the dynamics of a many particles system, one could calculate the force of each particle by considering the influence of each of its neighbors. In the dynamical calculation, with all the given initial velocities and positions, the future behavior of the system is determined using the potential at a point and Newton's second law. The MD model is used for studying the surface kinetics during the epitaxial growth, the dynamics of strained layer epitaxy and the evolution of the surface diffusion coefficient [61]. In the dynamical method, it is practical to follow a small system of molecules for only about one microsecond at low temperature. Another limitation of the method is to consider the smallness of the system studied. Only short range interaction between particles can be considered. The solution of the coupled equations of motion for any particle of the system in MD restricts the number of particles and also the range of real time simulation because of limitations in CPU time. The specific advantage of MD simulations is that the

surface kinetics can be studied to get atomic details [62].

Ashu *et al* [30] performed molecular dynamics simulation of $In_xGa_{1-x}As$ on substrate $GaAs(100)$ to show the dynamics of threading dislocations in the over layers and the formation of misfit dislocations at the heterojunction interface. They developed a code by using a modified Tersoff potential [31,32], which simulates the threading dislocation dynamics in the $InGaAs$ over layer, and also the formation of interface misfit dislocations. To completely simulate the $InGaAs$ structure, potential energy function PEF's for the $In-In$, $Ga-Ga$, $As-As$, $In-As$, $Ga-As$ and $In-Ga$ interactions are required. Following Smith [34], who used the functional form due to Tersoff [31,32], Ashu *et al* fitted PEF's for four of these types of interactions($In-In$, $Ga-As$, $In-As$ and $In-Ga$), using Smith's [34] parameters for the remaining two. The interaction energy between each bond is defined as V_{ij} for the i_{th} atom to the j_{th} atom. The functional form of the PEF's used is:

$$E = \sum_{i,j} V_{ij} \tag{2.11}$$

$$E = (\frac{1}{2}) \sum_{i,j} f_c(r_{ij})(A_{ij}e^{-\lambda_{ij}r_{ij}} - b_{ij}B_{ij}e^{-\mu_{ij}r_{ij}}) \tag{2.12}$$

The definition of b_{ij} and $f_c(r_{ij})$ have been described in literatures [30-34]. These relations are described as functions of r_{ij} and θ_{ijk}. r_{ij} are bond lengths of the ith atom to the jth atom and θ_{ijk} are the angles of three atoms i, j and k and each index runs from 1 to 3 for As, Ga and In, respectively. The constants A_{ij}, B_{ij}, λ_{ij} and μ_{ij} for the various interactions are shown in table by Ashu[30]. Ashu showed the formation of misfit dislocation for $In_xGa_{1-x}As/GaAs(100)$ systems. It was observed that continued deposition results in the excess strain being relieved by the formation and migration of defects. In the simulation of dislocations, the inner and boundary region atoms are placed according to the strain fields predicted by elasticity theory. In this simulation, the inner and boundary region atoms are placed according to the

strain fields predicted by elasticity theory. By using this method, a 45° dislocation strain field was imposed on the substrate and a 60° in the over layer [30].

The Stochastic model is based on the master equation approach with quasi-chemical approximation and the solid on solid restriction [48-49]. The time evolution of the epilayer is described by the rate of change of macrovariables of growth such as concentration of atoms, the atom-atom pair concentration of atom-vacancy pair concentrations. The model involves solving simultaneous non-linear differential equations and hence computationally less intensive but does not provide microscopic details of the atoms. The surface kinetic processes considered in this method are the relaxation processes such as the adsorption, the evaporation also the surface diffusion processes such as the intralayer and the interlayer diffusion. These models are studied with either pure relaxation kinetics or pure diffusion kinetics. Saito and Krumbhar (SK model) [48] studied the combined influence of the relaxation and the surface diffusion processes.

Venkatasubramanian [49] developed a stochastic model for the MBE growth kinetic studies of compound semiconductors based on the work of Saito *et al* [48]. The model developed at first for diamond cubic lattice and later for the two-sublattices zinc blende structure based on the master equation approach and modified solid-solid restriction. Therefore the atom is not absorbed exactly on top of another atom but in a vacant site whose projection falls in between a pair of nearest neighbor atoms. The time evolution of the epilayer is described by the rate of change of a complete set of macro variables such as coverage of atoms in a layer, atom-atom pair concentration etc. The kinetics of the low temperature $GaAs$ were studied using the modified model [51] which in addition to the surface processes like incorporation, evaporation and migration, included the kinetics of the physisorbed layer of As, loosely bound to the surface of the growing crystal by Van der Waals type binding. The thermally

activated surface processes are considered rate limiting to dictate the growth of the film.

The modified stochastic model developed by Muthuvenkatraman *et al* [52] considered the surface kinetics such as incorporation of arsenic from the physisorbed layer onto the substrate, the intra-layer migration, inter-layer migration and evaporation processes of the gallium arsenide. The antisites incorporation from the physisorbed arsenic (PA) layer and the evaporation of the antisites were studied and fitted to Arrhenius form of equations with incorporation lifetime τ_{in} and evaporation lifetime τ_{ev} factors and activation energies for incorporation and evaporation.

A rate equation model proposed by Krishnan *et al* [70] included the presence and dynamics of physisorbed arsenic (PA) riding the growth surface in the low temperature molecular beam epitaxy (MBE) of (100) gallium arsenide ($GaAs$). The model results for the dependence of As^{+}_{Ga} and As^{0}_{Ga} concentrations on beam equivalent pressure (BEP) and growth temperature agreed well with experiments [41]. Using the same kinetic model for the temporal behavior of the surface, the contribution of the PA layer to the reflection high energy electron diffraction (RHEED) intensity was computed based on kinematic theory of electron diffraction [51]. The results were in agreement with experimental results [40].

CHAPTER 3

THE THEORETICAL MODEL FOR MBE GROWTH DYNAMICS STUDIES

3.1 Introduction

In this chapter, a rate equation model was used in the MBE growth dynamics studies of compound semiconductors. The physical basis of the model includes several plausible surface kinetic processes and its mathematical formulation is in terms of first order non-linear differential equations. The numerical method to solve the first order differential equations, the fourth-order Runge-Kutta method, is also briefly described.

3.2 The Kinetic Rate Equation Model

The MBE growth simulation of $InGaAs$ on $GaAs$ [100] substrate was considered. Growth of compound semiconductors is a result of dynamic processes occurring on a surface riding physisorbed material layer (PM) and the surface of the crystalline epilayer. The PM layers may contain any or all of the species that are used in the growth. The atoms/molecules in this layer are physisorbed on to the surface by Van der Waals type binding. The PM layer undergoes several dynamic processes such as the adsorption of atom onto crystal, the evaporation of atom out of it into vacuum and the segregation of atoms from the crystal into the PM layer. The rates of these processes are assumed to be Arrhenius type with the form:

$$\tau_i = \tau_{o,i,e} e^{\frac{E_i}{kT}} \tag{3.1}$$

where $\tau_{o,i,e}$ is the time constant for the process 'i', E_i is the activation energy for the processes, k_B is Boltzmann constant, and T is temperature in Kelvin. Figure 4.1

depicts a schematic picture of the surface processes of the PM layer. The surface dynamic processes considered for the epilayer in the model are adsorption, evaporation, interlayer and intralayer migration, and segregation. The rate of adsorption depends on the flux rate and the availability of proper surface site with surface covalent bonds satisfaction. The segregation from the crystal layer is allowed only for In. The rate of evaporation and migration of atoms are modeled based on Arrhenius type rate equations with frequency factors and activation energies:

$$R = R_0 e^{\frac{-E_{act}}{k_B T}} \tag{3.2}$$

where R_0 is the frequency prefactor, E_{act} is the activation energy, k_B is the Boltzmann constant and T is the temperature in Kelvin. The atom interactions are assumed to be pairwise and only up to second nearest neighbor interactions are considered. The activation energy for the segregation process, i.e., from the crystal to the physisorbed state, is assumed to be smaller than that for the evaporation process, but larger than that of the surface migration process.

The time evolution of the growing epilayer is described through the change of macro variables resulting from the surface processes. The macro variables of growth are normalized with respect to the maximum number of possible atoms in the layer. The macro variables considered are the layer coverages of Ga, As, and In in their respective layers and are given as:

$$\begin{aligned} C_{Ga}(2n) &: \text{layer coverage of } Ga \text{ in the } 2n^{th}\text{layer} \\ C_{As}(2n+1) &: \text{layer coverage of } As \text{ in the } 2n+1^{th}\text{layer} \\ C_{In}(2n) &: \text{layer coverage of } In \text{ in the } 2n^{th}\text{layer} \\ \text{PM layer coverage} &, \quad C_{Ga}^{PM}, C_{As}^{PM} \text{ and } C_{In}^{PM} \end{aligned} \tag{3.3}$$

where n is the layer index, with the regular Ga and In belonging to even numbered layers, and the regular As belonging to the odd numbered layers. The layer coverage

of atoms is 1 when the layer is completely full and 0 when the layer is completely empty. Only a monolayer of the PM layer will be exposed to that epilayer surface, and hence is dynamically active. Therefore, a constraint on the PM layer coverage is $C_{Ga}^{PM} + C_{As}^{PM} + C_{In}^{PM} \leq 1.0$. The time evolution of the layer coverage of Ga in the $2n^{th}$ layer due to the various surface processes is given by:

$$\begin{aligned}
\frac{dC_{Ga}(2n)}{dt} &= \left([C_{As}(2n-1) - C(2n)]\,(J_{Ga} + \frac{C_{Ga,phy}}{\tau_{in}^{Ga}})\right)(A1) + [C_{As}(2n-1) - C(2n)] \\
&\times \left(R_0 e^{\frac{-E_{d,Ga}(2n+2)}{kT}} \left(\frac{C_{Ga}(2n+2)}{C(2n+2)}\right)[C(2n+2) - C_{As}(2n+3)]\right. \\
&+ \left. R_0 e^{\frac{-E_{d,Ga}(2n-2)}{kT}} \left(\frac{C_{Ga}(2n-2)}{C(2n-2)}\right)[C(2n-2) - C_{As}(2n-1)]\right)(B1) \\
&- R_0 e^{\frac{-E_{d,Ga}(2n)}{kT}} \left(\frac{C_{Ga}(2n)}{C(2n)}\right)[C(2n) - C_{As}(2n+1)] \\
&\times ([C_{As}(2n+1) - C(2n+2)] + [C_{As}(2n-3) - C(2n-2)])\,(C1) \\
&- R_0 e^{\frac{-E_{e,Ga}(2n)}{kT}} \left(\frac{C_{Ga}(2n)}{C(2n)}\right)[C(2n) - C_{As}(2n+1)]\,(D1) \qquad (3.4)
\end{aligned}$$

where the term $A1$ denotes the increase in $C_{Ga}(2n)$, due to adsorption of Ga from the incoming molecular beam. The rate of adsorption is the product of the available sites for Ga incorporation on the surface, $[C_{As}(2n-1) - C(2n)]$, and the fluxes of Ga, J_{Ga} from the molecular beam and $\frac{C_{Ga,phy}S_1}{\tau_{in}^{Ga}}$ from the PM layer. The sticking coefficient of Ga is taken as unity. The term $B1$ describes the increase in $C_{Ga}(2n)$ due to migration into the $2n^{th}$ layer from adjacent Ga layers indexed $(2n+2)$ and $(2n-2)$ and fraction of available sites for Ga in the $2n^{th}$ layer is $[C(2n-2) - C_{As}(2n-1)]$. The rate of migration is described by Arrhenius type rate equations with frequency factor, R_0, and activation energy, E_d. The cation sublattice contains two possible elements, Ga and In. Thus, the layer coverages satisfy:

$$C(2n+2) = C_{Ga}(2n+2) + C_{In}(2n+2)$$

of the fraction of the $(2n+2)^{th}$ layer exposed, only a portion of it belongs to Ga. Thus, the fraction $\frac{C_{Ga}(2n+2)}{C(2n+2)}$ is used to make sure that only the Ga portion is considered for

migration. Similar arguments hold for the $(2n-2)^{th}$ layer also. The activation energy for a particular layer is a function of layer coverage of that layer, the activation energies of isolated atoms, $E_{d,iso}$, and the second neighbor atom-atom pair interaction energy, E_{GaGa}, and E_{InGa}. The factor of four is used to allow for four possible neighboring atoms. In the mathematical form, the activation energy for Ga diffusion for the $(2n-2)^{th}$, layer is given as:

$$E_{d,Ga}(2n-2) = E_{d,Ga,iso} + 4E_{GaGa}C_{Ga}(2n-2) + 4E_{GaIn}C_{In}(2n-2)$$

Thus $E_{d,Ga}(2n-2)$ is equal to $E_{d,Ga,iso}$, when the coverage is very small. Its value is given by above equation with $C_{In}(2n-2)+C_{Ga}(2n-2) = 1.0$, when the layer is full. The term $C1$ denotes the decrease in $C_{Ga}(2n)$ due to migration of Ga out of the $2n^{th}$ layer to the adjacent layers, $(2n+1)$ and $(2n-3)$. The description of the rate of this process is similar to term $B1$, with $E_d(2n)$ being the activation energy for migration from the $2n^{th}$ layer, $[C_{As}(2n+1) - C(2n+2)]$ and $[C_{As}(2n-3) - C(2n-2)]$ being the fractions available Ga atoms for migration into the adjacent layers (2n+1) and $(2n-3)$, respectively. $\frac{C_{In}(2n)}{C(2n)}[C_{As}(2n) - C(2n+1)]$ is the fraction of Ga atoms in the $2n^{th}$ layer. The value of $E_{d,In,iso}$, E_{InIn} and E_{GaIn} are in Table 4.1. The term $D1$ describes the evaporation of Ga atoms from the $2n^{th}$ layer resulting in the decrease in $C_{Ga}(2n)$ with activation energy for evaporation, $E_{e,Ga}(2n)$ and the fraction of the $2n^{th}$ layer exposed, $\frac{C_{Ga}(2n)}{C(2n)}[C_{As}(2n) - C(2n+1)]$.

The description of the activation energy for evaporation, $E_{e,Ga}$, is similar to that of $E_{d,Ga}$ and is written as:

$$E_{e,Ga}(2n) = E_{e,Ga,iso} + 4E_{GaGa}C_{Ga}(2n) + 4E_{GaIn}C_{In}(2n)$$

with $E_{e,Ga,iso}$ is the evaporation energy for the isolated Ga atom. The description of the activation energy for segregation, $E_{s,In}$ is similar to that of $E_{d,Ga}$ and is written

as:

$$E_{s,In}(2n) = E_{s,In,iso} + 4E_{InIn}C_{In}(2n) + 4E_{InGa}C_{Ga}(2n) \quad (3.5)$$

with $E_{s,In,iso}$ is the segregation activation energy for the isolated In atom. Equations similar to Eqn. (3.4) are written for Ga in the $2n^{th}$ layer and As in the $(2n+1)^{th}$ layer. In our model, all the parameters including the incorporation rate from the physisorbed As state are kept identical for both As_4 and As_2 fluxes to make the model simple. The time evolution of the layer coverage of In in the $2n^{th}$ layer is written as:

$$\begin{aligned}
\frac{dC_{In}(2n)}{dt} &= \left([C_{As}(2n-1) - C(2n)]\,(J_{In} + \frac{C_{In,phy}}{\tau_{in}^{In}})\right)(A2) + [C_{As}(2n-1) - C(2n)] \\
&\times \left(R_0 e^{\frac{-E_{d,In}(2n+2)}{kT}}\left(\frac{C_{In}(2n+2)}{C(2n+2)}\right)[C(2n+2) - C_{As}(2n+3)]\right. \\
&+ \left. R_0 e^{\frac{-E_{d,In}(2n-2)}{kT}}\left(\frac{C_{In}(2n-2)}{C(2n-2)}\right)[C(2n-2) - C_{As}(2n-1)]\right)(B2) \\
&- R_0 e^{\frac{-E_{d,In}(2n)}{kT}}\left(\frac{C_{In}(2n)}{C(2n)}\right)[C(2n) - C_{As}(2n+1)] \\
&\times ([C_{As}(2n+1) - C(2n+2)] + [C_{As}(2n-3) - C(2n-2)])\,(C2) \\
&- R_0 e^{\frac{-E_{e,In}(2n)}{kT}}\left(\frac{C_{In}(2n)}{C(2n)}\right)[C(2n) - C_{As}(2n+1)]\,(D2) \\
&- R_0 e^{\frac{-E_{s,In}(2n)}{kT}}\left(\frac{C_{In}(2n)}{C(2n)}\right)[C(2n) - C_{As}(2n+1)]\,(E2) \quad (3.6)
\end{aligned}$$

Note that Eqn. (3.6) is similar to (3.4) except for the substitution of Ga with In. The activation energies $E_{d,In}$ and $E_{e,In}$ are given by:

$$E_{d,In} = E_{d,In,iso} + 4E_{InIn}C_{In} + 4E_{GaIn}C_{Ga}$$

and

$$E_{e,In} = E_{e,In,iso} + 4E_{InIn}C_{In} + 4E_{GaIn}C_{Ga},$$

respectively. The description of terms $A2$, $B2$, $C2$ and $D2$ are similar to that of $A1$, $B1$, $C1$ and $D1$ except the substitution of Ga with In and the last term $E2$ related to In segregation to the PM layer..

The time evolution of the layer coverage of As in the $(2n+1)^{th}$ layer, $C_{As}(2n+1)$, is written as:

$$\begin{aligned}
\frac{dC_{As}(2n+1)}{dt} &= \left([C(2n)-C(2n+1)]\,(J_{As}+\frac{C_{As,phy}}{\tau_{in}^{As}})\right)(A3)+[C(2n)-C(2n+1)] \\
&\times \left(R_0 e^{\frac{-E_{d,As}(2n+3)}{kT}}\left(\frac{C_{As}(2n+3)}{C(2n+3)}\right)[C(2n+3)-C(2n+4)]\right. \\
&+ \left. R_0 e^{\frac{-E_d(2n-1)}{kT}}\left(\frac{C_{As}(2n-1)}{C(2n-1)}\right)[C(2n-1)-C(2n)]\right)(B3) \\
&- R_0 e^{\frac{-E_d(2n+1)}{kT}}\left(\frac{C_{As}(2n+1)}{C(2n+1)}\right)[C(2n+1)-C(2n+2)] \\
&\times ([C(2n+2)-C_{Ga}(2n+3)]+[C(2n-2)-C(2n-1)])\,(C3) \\
&- R_0 e^{\frac{-E_e(2n+1)}{kT}}\left(\frac{C_{As}(2n+1)}{C(2n+1)}\right)[C(2n+1)-C(2n+2)]\,(D3) \qquad (3.7)
\end{aligned}$$

Terms $A3$, $B3$, $C3$ and $D3$ are similar to those of Eqn. (3.4).

Thus, coupled nonlinear first order differential equations given by Eqn. (3.4), (3.6) and (3.7) are obtained from the time evolution of all the macro variables for every layer. These equations are simulated with additional equations for describing the dynamics of Ga, In and As in the PM layer. The time evolution of the PM layer coverage of i^{th} species, $\frac{dC_i}{dt}$, is given by:

$$\begin{aligned}
\frac{dC_{i,phy}}{dt} &= (J_i(1-S_1))-\frac{C_{i,phy}}{\tau_{ev}^i}-\frac{C_{i,phy}S_1}{\tau_{in}^i} \\
+R_0 e^{\frac{E_s(2n)}{kT}} &\sum_{\text{all layers}}\left(\frac{C_i(2n)}{C(2n)}\right)[C(2n)-C_{As}(2n+1)] \qquad (3.8)
\end{aligned}$$

where i represents either Ga or In except that there is no segregation of Ga from the crystal which is given by the last term on the RHs. A similar equation is written for physisorbed As without the segregation term and the As getting incorporated in to the anion sublattice. The sum of the coverage of Ga, In and As are not exceeded than 1 as only a monolayer coverage of the PM layer is effective in the surface dynamics. J_i is the molecular flux of i^{th} coming onto the substrate and its unit here is in atom/sec. The unit of flux is usually in atoms/cm^2.sec. and it can be

converted to atom/site.sec. which is simply written as atom/sec. The conversion is performed using the effective area per crystalline site which in case of $GaAs$ substrate with lattice constant a=5.6533Å, is given by $a^2/2$ and is equal to 15.97Å^2 in the (100) growth direction. In the above equation, the first term denotes the increase in PM coverage due to arrival of i^{th} species flux into the PM layer. The next two terms denote the net loss of the PM layer coverage due to evaporation and chemisorption in to the appropriate site, respectively. The last term is gain of the PM layer coverage due to the segregation of atoms from the crystal which applies only to In. The various τ's are the time constants representing the respective surface processes. S_1 in Eqn. (3.8) represents the total fraction of the appropriate surface available for the incorporation of atoms.

3.3 Runge-Kutta Method

Runge-Kutta method [68] is one of the Euler methods to solve differential equations. It is a numerical method that requires only the initial points in order to begin the algorithm and improve the solutions. Consider the simple case of a single first-order differential equation, $dy/dt = f(y,t)$. The values at time step 'i', y_i and t_i, are given. The goal is to extrapolate across the time interval Δt to estimate the values at step $i+1$. In order to carry out this extrapolation, the Runge-Kutta scheme first estimates where the center of the interval is located. The value of t at the center is, $t_i + \Delta/2$. The Runge-Kutta algorithm, then, evaluates the slope of the function at the mid point of the interval and uses this slope to extrapolate all the way across the interval. The corresponding equations are:

$$k_1 = f(y_i, t_i)\Delta t$$

$$k_2 = f(y_i + k_1/2, t_i + \Delta t/2)\Delta t$$

$$y_{i+1} = y_i + k_2$$

In other words, $y_i + k_1/2$ is the Euler estimate for y at the center of the interval and $k_2/\Delta t$ is the slope at the center. The error in this estimate for y_{i+1} is proportional to $(\Delta t)^3$, in contrast to the Euler method for which it is on the order of $(\Delta t)^2$. Hence, in this sense the Runge-Kutta method more accurate than the Euler method. The most commonly used Runge-Kutta method is the one comes from the Taylor expansion of $y(t + \Delta t)$. For simplicity let $\Delta t = \tau$. The accuracy of the method is higher with considering higher degree of τ. The Taylor expansion is given as:

$$y(t+\tau) = y(t) + \tau\dot{y} + \frac{\tau^2}{2}\ddot{y} + \frac{\tau^3}{3!}y^{(3)} + \cdots$$

$$y(t+\tau) = y(t) + \tau g + \frac{\tau^2}{2}(g_t + g g_y) + + \frac{\tau^3}{6}(g_{tt} + 2g g_{ty} + g^2 g_{yy} + g g_y^2 + g_t g_y + \cdots$$

where the indices are for partial derivatives. For example, $g_{yt} = \partial^2 g/\partial y \partial t$. one can also write the solution at $t + \tau$ as:

$$y(t+\tau) = y(t) + \alpha_1 k_1 + \alpha_2 k_2 + \alpha_3 k_3$$

with

$$k_1 = \tau g(y, t)$$

$$k_2 = \tau g(y + \beta_{21} k_1, t + \beta_{21}\tau)$$

$$k_3 = \tau g(y, t\beta_{31} k_1 + \beta_{32} k_2, t + \beta_{31}\tau + \beta_{32}\tau)$$

for the expansion of the term $O(\tau^3)$. The flexibility in choosing the parameters $(\beta_{21}, \beta_{31}, ...)$ provides one more way to increase the numerical accuracy in practice. The most common fourth-order Runge-Kutta algorithm which truncated Taylor expansion at the term $O(\tau^4)$, is given by:

$$y(t+\tau) = y(t) + \frac{1}{6}(k_1 + 2k_2 + 2k_3 + k_4)$$

where

$$k_1 = \tau g(y, t)$$

$$k_2 = \tau g(y + \frac{k_1}{2}, t + \frac{\tau}{2})$$

$$k_3 = \tau g(y + \frac{k_2}{2}, t + \frac{\tau}{2})$$

$$k_4 = \tau g(y + k_3, t + \tau)$$

where $y = g(y, t)$. The above solution of parameters satisfies the required equations. This algorithm can be modified according to the problem under study.

3.4 Computational Details

Description of evolution of each bilayer of $InGaAs$ requires three first order nonlinear differential equations, one of which describing the time evolution of each of the normalized macro variables. In this work, simultaneous growth of 80 bilayers and the PA layer are considered, requiring a total of 243 (= 80 × 3 + 3) coupled nonlinear first order differential equations. The system of equations were integrated using the Fourth-order Runge Kutta method described in section (3.3) with time steps of less than 10^{-6} s to get the values of each of the macro variables as a function of time, for a growth time of 10 seconds. The growths were simulated on the Silicon Graphics supercomputer ORIGIN-2000. The average coverage of Ga, As and In in individual layers and the PM layers at the end of growth are obtained from the solution of the differential equations. A fraction of layer coverage of the particular species is obtained by this method.

3.5 Conversion of J_{As} to BEP

Experimentally, the As flux is described in terms of BEP for a given Ga flux, whereas our model requires the flux in number of monomer atoms per site per second. The conversion between the two flux definitions is accomplished using the following

equation :

$$\frac{J_{As_4}}{J_{Ga}} = \frac{P_{As_4}}{P_{Ga}} \frac{\eta_{Ga}}{\eta_{As_4}} \sqrt{\frac{T_{As_4}}{T_{Ga}} \times \frac{M_{Ga}}{M_{As_4}}} \tag{3.9}$$

where $\frac{P_{As_4}}{P_{Ga}}$ is the BEP, J is the flux and T is the absolute temperature and M is the molecular weight. η is the ionization efficiency for the respective species relative to nitrogen and is given by:

$$\frac{\eta}{\eta_{N_2}} = \left[\left(\frac{0.4Z}{14}\right) + 0.6\right] \tag{3.10}$$

where η_{N_2} is the ionization efficiency of diatomic nitrogen and Z is the atomic number. In Eqn. (3.9), the As is assumed to be a tetramer. The values used for MBE growth of $GaAs$ are: Z_{Ga}=31; Z_{As_4}=4×33; T_{As_4}= 1173°K; T_{Ga}=573°K; M_{Ga}=69.72 and M_{As_4}=4×74.92. The number of sites per cm^2 in case of (100) $GaAs$ is obtained as 1μm/hrs. = 2.77 Å/sec.; since one bilayer of $GaAs$ is half of the cubic lattice constant equal to 2.82 Å, then 1μm/hrs. = 0.98 atoms/site.sec. The equivalent surface area for a (100) site is 6 x 10^{-16}cm^2 and hence, the number of sites per cm^2 is obtained as 6.26×10^{14}. Using the conversion factors described in the above paragraph along with Eqn. (3.10), Eqn. (3.11) can be rewritten as:

$$J_{As}(\text{monomer/cm}^2\text{.sec.}) = 4.0 \times 1.46 \times 10^{14} \times \left(\frac{P_{As_4}}{P_{Ga}}(\text{BEP})\right) J_{Ga}(\mu\text{m/hrs.}) \tag{3.11}$$

where 4 is used for converting the tetramer to monomer. In the growth simulations, composition, indium flux J_{In} and gallium flux J_{Ga} were kept the same as the experimental data. To convert the As_4 and As_2 BEP's to fluxes (monomer/sec.), the following equations were used:

$$J_{As_4} = 0.2359 \times (BEP) \times J_{Ga} \tag{3.12}$$

and in the case of As_2:

$$J_{As_2} = 0.58526 \times (BEP) \times J_{Ga} \tag{3.13}$$

where BEP is the V/III ratio.

CHAPTER 4

RESULTS AND DISCUSSION

4.1 Model Parameter Fitting Procedure

The model involves several parameters such as time constants and activation energies, which are initially unknown. These unknown parameters are established according to the following procedure. Experimental conditions employed by Fournier *et al* [1] were simulated and the model parameters were adjusted systematically until In incorporation coefficient values for substrate temperature 803 and 903°K fitted well with the experimental data for a As_4 BEP of 36. Once the parameters were established, these parameters were used for the rest of the simulations with As_4 and As_2 at growth conditions employed by several independent research groups [1,3,7,8,17]. Detailed descriptions of these parameters and their values are discussed below.

The activation energy for incorporation processes of Ga and As from the PM layer to the crystal surface are assumed to be independent of temperature (i.e., E_{in}^{Ga}=0.0 eV and E_{in}^{As}=1.0 eV). The activation energy for the incorporation of In from the PM layer onto the crystal, E_{in}^{In} is assumed to be linearly dependent on the In coverage in the physisorbed layer and is given by:

$$E_{in}^{In} = 0.5 C_{In,phy} \tag{4.1}$$

where $C_{In,phy}$ is the coverage of In in the PM layer. Similarly the activation energies for the In, Ga and As evaporation process from the PM layer, E_{ev}^{In}, E_{ev}^{Ga} and E_{ev}^{As} are assumed to be linearly dependent on their own coverage in the physisorbed layer and are given by:

$$E_{ev}^{In} = 0.18 + 0.06C_{In,phy}$$
$$E_{ev}^{Ga} = 0.18 + 0.06C_{Ga,phy}$$
$$E_{ev}^{As} = 0.18 + 0.06C_{As,phy}$$

The prefactor of time constants for incorporation and evaporation processes are obtained according to the Arrhenius equation and related to the activation energies which were described earlier in Eqn. (3.1).

The evaporation, segregation and diffusion processes in the surface of the epilayer are assumed to be thermally activated and are modeled with the frequency factor, R_0 and activation energy given by Eqn. (3.2). R_0 is also linearly dependent on the substrate temperature, and is given by:

$$R_0 = 2.08 \times 10^{10} \times T$$

This is based on the phonon frequency obtained using the equi-partition energy principle. The frequency prefactor of diffusion processes are assumed constants. The frequency prefactor of In segregation is considered to be linearly dependent on the substrate temperature, and is given by:

$$R_{0,s} = 1.743 \times 10^{10} \times T$$

The segregation process from the PM layer is allowed only for In. It is noted that $R_{0,s}$ is smaller than the R_0 of evaporation and diffusion. All the model parameters and their dependences on the surface coverage are summarized in Table 4.1.

4.2 InGaAs Segregation and Desorption Studies

For this study, the growth conditions of Fournier *et al* [1] were used. The fluxes were: J_{Ga}=0.714 μm/h; J_{In}=0.192 μm/h; J_{As4} and J_{As2} BEP in the range of 17 to

36. The substrate temperature was in the range of 500-700°C. The In incorporation coefficient, which is defined as a ratio of the total In incorporated to the total In deposited, was obtained for various growth temperature for both As_4 and As_2 for a BEP of 36. Plots of In incorporation coefficient versus substrate temperature obtained from simulation are shown in Figure 4.2 along with the experimental results of Fournier *et al* [1]. The agreement is excellent for As_4 and fair for As_2 for entire temperature range. It is noted that there is no difference between the model parameters for As_4 and As_2. The In incorporation decreases with temperature for both As_4 and As_2 due to increased segregation of In to the PM layer and evaporation of In to the vacuum. The In incorporation coefficient is larger for As_2 than As_4 at the same BEP. The primary reason for this is that the actual flux of As monomer/ site.sec. for As_2 is more than that of As_4 given by Eqns.(3.12) and (3.14). Thus, in our model, no difference in reactivity between As_4 and As_2 is considered which makes the model simple to use.

Plots of In incorporation coefficient versus temperature for As_4 BEP of 17 along with the experimental results of Fournier *et al* [1] are shown in Figure 4.3. The agreement between the results in excellent below 570°C. Above 570°C, simulation results are lower than the experimental values but agree well with the values for BEP of 36. The experimental values saturate at 0.2, even though the physical reasons suggest that at 630°C, it should be close to zero, especially since the incorporation coefficient is close to zero for BEP 36.

Plots of In incorporation coefficient versus temperature are shown for various As_4 BEPs in Figure 4.4. As BEP increases, the incorporation coefficient increases due to reduced lifetime for In surface atoms for the evaporation and segregation processes. It is observed that to achieve a high In incorporation a low substrate temperature below 570°C and high BEP of As_4 above 17 are needed.

Desorption parameter of the i^{th} species, D_i, was found as the difference between the arriving atoms and the change in the total atom concentration in the crystal and the PM layer in a preset short period of time. Mathematically, it can be written as:

$$D_i = J_i(\Delta t - \left[\sum_{\text{all grown layers}} [C_i(2n)(t+\Delta t) - C_i(2n)(t)]\right]) - [C_{i,phy}(t+\Delta t) - C_{i,phy}(t)] \tag{4.2}$$

where Δt was arbitrarily chosen as 0.1 s for the simulation. The In and Ga fluxes were on from 0 to 5 s and at 5 s, the In flux was terminated. Plots of In desorption parameters, D_{In}, (computed using Eqn. (4.2)) versus time for a As_4 BEP of 36 is shown in Figure 4.5. These results agree qualitatively well with the experimental results of Ref.[1]. A quantitative comparison can not be made due to the arbitrary nature of the experimental results. The In desorption rate initially increases rapidly and reaches a steady state within 2 s. After the In flux is terminated, the In desorption flux decreases exponentially to zero. As expected, the desorption rate is larger for higher temperatures. Additionally, D_{In} shows periodic oscillations in the desorption flux which is related to the periodic exposure of the cation and anion layers due to layer-by-layer evaporation from the crystal. Even though there are noticeable oscillations in the experimental data [1], it is not as periodic as our results.

Indium desorption parameters versus time is shown in Figure 4.6 for 903°K for As_4 BEPs of 36 and 17. The indium desorption for higher BEP is larger which agrees qualitatively with Fourier *et al.* The reason for this behavior is that at high BEP, the coverage of As in the PM layer increases which causes decreasing the coverage of In in the PM layer. Thus less In incorporates in to the crystal. In other words more In adsorbs.

Relative desorption parameter (RDP) is defined as the ratio of steady state the desorption parameter $D_{In}(T)$ to $D_{In}(803^oK)$ where 803°K is the lowest temperature in our study. RDP was obtained for several temperatures from Figure 4.5 for a As_4

BEP of 36. A plot of RDP versus substrate temperature is shown that along with the experimental data of Fournier *et al* is shown in Figure 4.7. The agreement between the results is excellent for most of the temperature range. Experimental [1] as simulation plots of RDP versus temperature for a As_4 BEP of 17 shown in Figure 4.8 also shows good agreement.

The MBE growth simulation was also performed for $GaAs$ growth experiments of Kao *et al* [8]. Simulated gallium desorption parameters, D_{Ga} given by equation similar to Eqn. (4.2) in the presence of As_4 flux is shown in Figure 4.9. The activation energy for desorption was found 2.92 eV from Figure 4.9. This value of 2.92 eV is smaller than that obtained by Kao *et al* [8]. But our value is reasonable, considering the fact that a surface Ga surrounded by four in-plane Ga neighbors will have an activation energy of about 3.5 eV and a Ga is surrounded by by two in-plane Ga atoms will have about 3.1 eV.

Our investigations strengthened the previous suggestions in the literature [1] that there are two components to the desorption process, one from the surface riding In and the other from the crystal. The activation energy for these processes for an isolated adatom are 0.18 eV and 2.6 eV, respectively. Plots of In layer composition versus layer number is shown in Figure 4.10 for various substrate temperature at a BEP of 36. The growth simulation were performed for 10 s at a growth rate of 0.912 ML/s. These results agree fairly well with the experimental results of Ref. [8]. At lower temperatures the In composition unform over 10 layers for most temperatures. The segregation of In spreads over at least 10 layers which suggests that these will considerable roughness of alloy mixing at heterointerfaces.

Segregation coefficient, R, can be obtained using Eqn. (2.1) and data Figure 4.10 following equation:

$$logR = \frac{1}{n} log\left(1 - \frac{x_n}{x_o}\right) \tag{4.3}$$

where n is the number of the layer and x_o and x_n are the nominal composition and the composition of the n^{th} layer, respectively. Plots of R versus temperature obtained for several BEPs of As_2 and As_4 is shown along with the experimental data of Kao *et al* [8] for As_4 BEP of 6 in Figure 4.11. Qualitatively, the results are in good agreement. In general, the segregation coefficient, R increases non-linearly with temperature and attains a maximum value of 1.0 at 850°K for a As_4 BEP of 17. The temperature at which the maximum R is attained increases with BEP as segregation rate decreases with BEP.

4.3 General Observations and Growth Implications

- The In incorporation to the surface layer decreases in substrate temperature higher than 540°C, more indium atoms incorporate to the the growth surface when the BEP ratio is higher than 20.

- The In segregation rate is large for higher temperatures and low As over-pressure. Thus, to minimize the In segregation, one should adopt lower temperatures and high As over-pressures. But, the temperature should not be set so low that the other thermally activated surface processes such as migration and As molecular adsorption by reaction are suppressed.

- The In desorption for BEP of 36 has a higher rate compare to 17, the actual desorption ratio shows the same behavior in experiment and simulation, it goes up more rapidly by increasing substrate temperature when BEP is higher.

- In desorption has two components, one from the surface riding In layer and the other from the surface of the crystal itself. The former component is smaller

than the latter.

- As_2 limits the In segregation rate more As_4 of the same BEP and it appears that As_2 is a better choice for limiting In segregation. Therefore, cracked As_4 should be employed.

- The simulated In composition versus growth monolayer number shows that the In segregation for substrate temperature range 803-903°K, starts at the 4^{th} monolayer and increases by increasing the number of layers.

- For lower As BEP, In segregation occurs at lower temperatures.

4.4 Advantages and Limitations of the Model

The kinetic rate equation model developed calculates the change in concentration of elements in each epilayer grown at each interval of time. Since the model is described by a system of differential equations, the calculations can be performed easily with less computational time. The model considers surface kinetic processes like incorporation, evaporation, migration, deposition, nucleation, growth of islands and interlayer and intralayer migration of atoms from the islands. The model is simple and not limited by crystal size. The doping kinetics in the crystal growth can be performed with ease. Any number of elemental sources can be considered with all surface processes applicable. The main disadvantage of the model is that the microscopic details of the atoms, such as size and shape of the islands, cannot be obtained. The position of atoms or the energy cannot be determined and hence the sites available for antisites are considered only from the total number of atoms in the layer. The activation energies for evaporation, E_e and migration, E_d considered with four neighbor atoms is only approximate and the energies may be a different function of the coverage of atoms.

Table 4.1: Fitted model parameters such as energies, time constants and frequency factors and their dependences

Symbol	Description	Model Value
$\tau_{0,in}^{Phy,Ga}$	prefactor for physisorbed *Ga* incorporation	10^{-3}s
$\tau_{0,in}^{Phy,As}$	prefactor for physisorbed *As* incorporation	10.0 s
$\tau_{0,in}^{Phy,In}$	prefactor for physisorbed *In* incorporation	0.2 s
$\tau_{0,ev}^{Phy,Ga}$	prefactor for physisorbed *Ga* evaporation	100.0s
$\tau_{0,ev}^{Phy,As}$	prefactor for physisorbed *As* evaporation	10^{-4}s
$\tau_{0,ev}^{Phy,In}$	prefactor for physisorbed *In* evaporation	10^{3}s
$R_0^{d,Ga}$	frequency factor for *Ga* for diffusion	2.4 X 10^{8}/s.
$R_0^{d,As}$	frequency factor for *As* for diffusion	4.38 X 10^{7}/s.
$R_0^{d,In}$	frequency factor for *In* for diffusion	4.38 X 10^{5}/s.
E_{in}^{Ga}	activation energy for incorporation of *Ga*	0.0 eV
E_{in}^{As}	activation energy for incorporation of *As*	1.0 eV
E_{in}^{In}	activation energy for incorporation of *In*	0.5 C_{In}^{phy} eV
E_{Ga-Ga}	2^{nd} neighbor atom-atom pair interaction energy for Ga	0.188 eV
E_{As-As}	2^{nd} neighbor atom-atom pair interaction energy for As	0.188 eV
E_{Ga-In}	1^{st} neighbor atom-atom pair interaction energy for Ga-In	0.0 eV
E_{In-In}	2^{nd} neighbor atom-atom pair interaction energy for In	0.173 eV
E_{Ga-As}	1^{st} neighbor atom-atom pair interaction energy for Ga-As	0.94 eV
E_{In-As}	1^{st} neighbor atom-atom pair interaction energy for In-As	0.86 eV
$E_{d,iso}^{Ga}$	activation energy for diffusion for isolated Ga atom	1.2 eV
$E_{d,iso}^{In}$	activation energy for diffusion for isolated In atom	1.3 eV
$E_{d,iso}^{As}$	activation energy for diffusion for isolated As atom	1.2 eV
$E_{e,iso}^{Ga}$	evaporation activation energy for isolated Ga atom	2.63 eV
$E_{e,iso}^{In}$	evaporation activation energy for isolated In atom	2.13 eV
$E_{e,iso}^{As}$	evaporation activation energy for isolated As atom	2.63 eV
E_{ev}^{Ga}	activation energy for the Ga evaporation	0.18+0.06C_{Ga}^{phy*} eV
E_{ev}^{In}	activation energy for the In evaporation	0.18+0.06C_{In}^{phy**} eV
E_{ev}^{As}	activation energy for the As evaporation	0.18+0.06C_{As}^{phy***} eV
$E_{s,In,iso}$	segregation activation energy for the isolated In atom	2.1 eV

* C_{Ga}^{phy}-Ga coverage in the physisorbed layer

** C_{In}^{phy}-In coverage in the physisorbed layer

*** C_{As}^{phy}-As coverage in the physisorbed layer

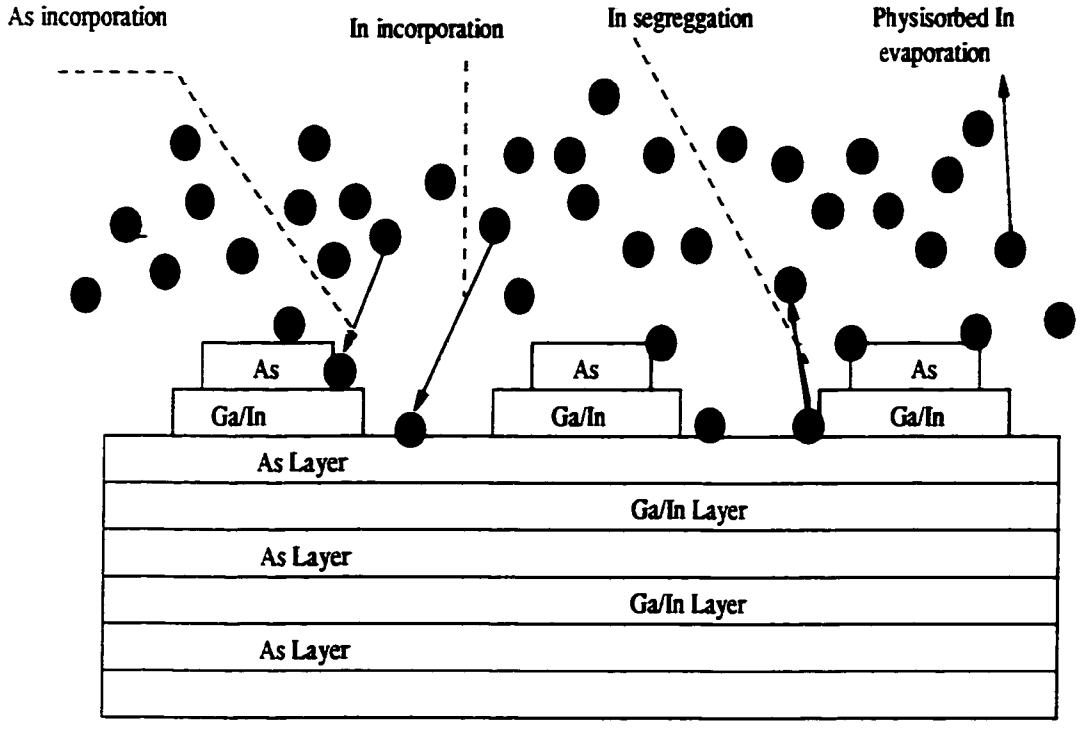

Figure 4.1: A schematic picture of the surface processes in MBE growth of InGaAs.

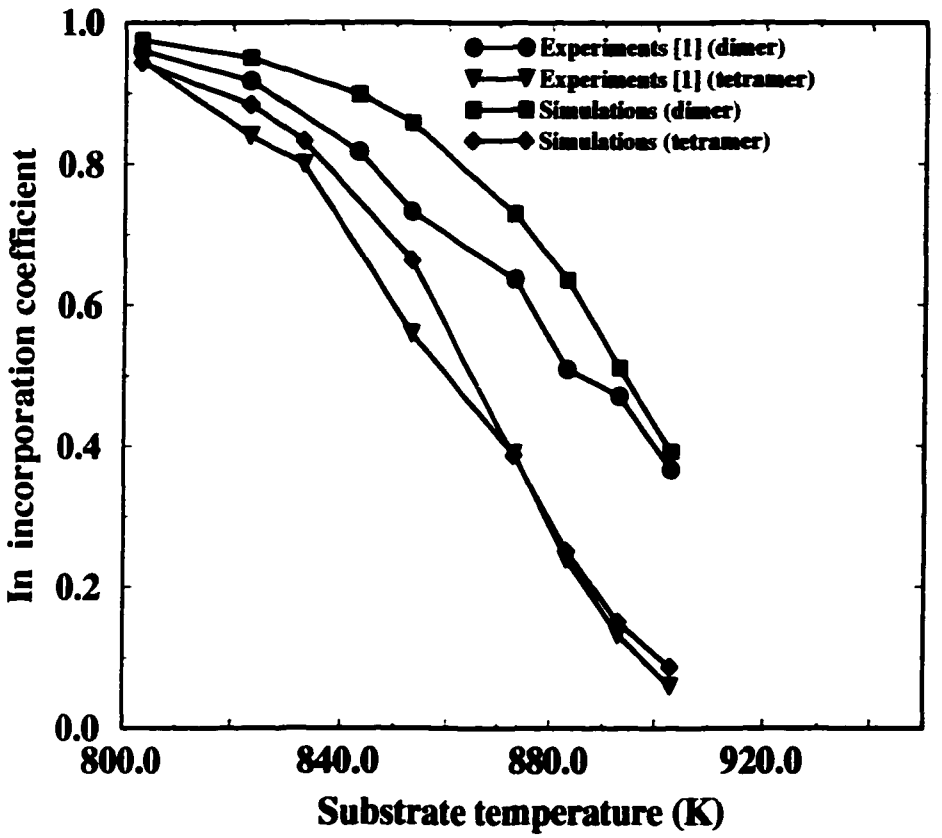

Figure 4.2: Comparison between experimental [1] and simulated results for In incorporation coefficient versus substrate temperature for a BEP of 36 with As_2 and As_4 fluxes.

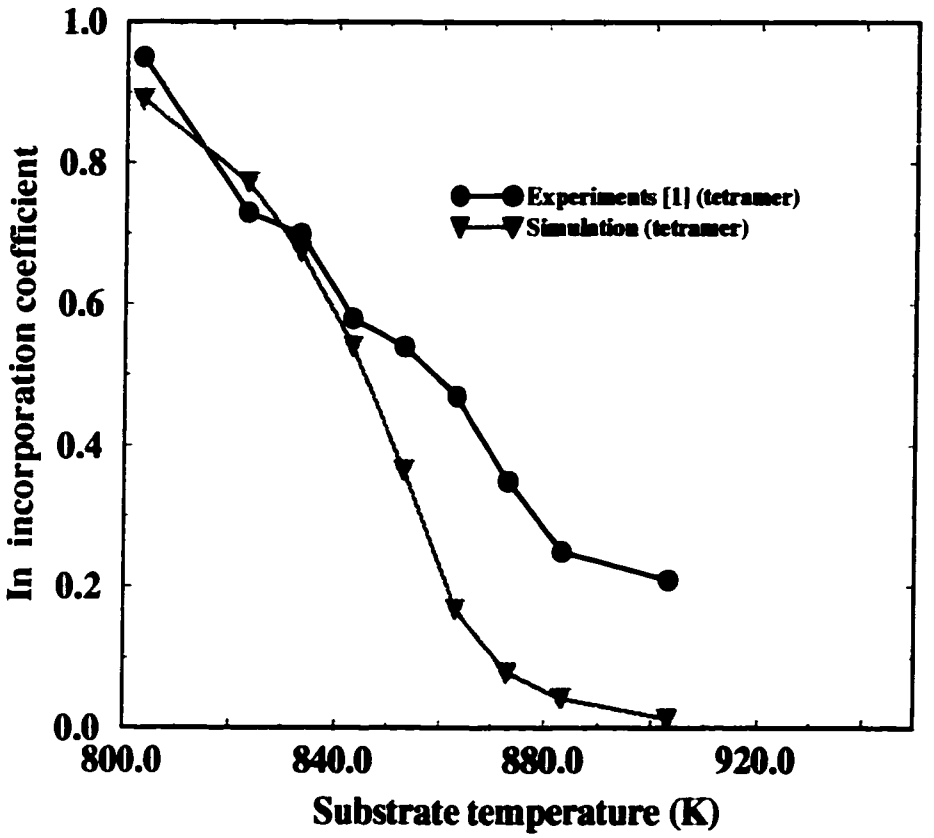

Figure 4.3: Comparison between experimental [1] and simulated results for In incorporation versus substrate temperature for a As_4 BEP of 17.

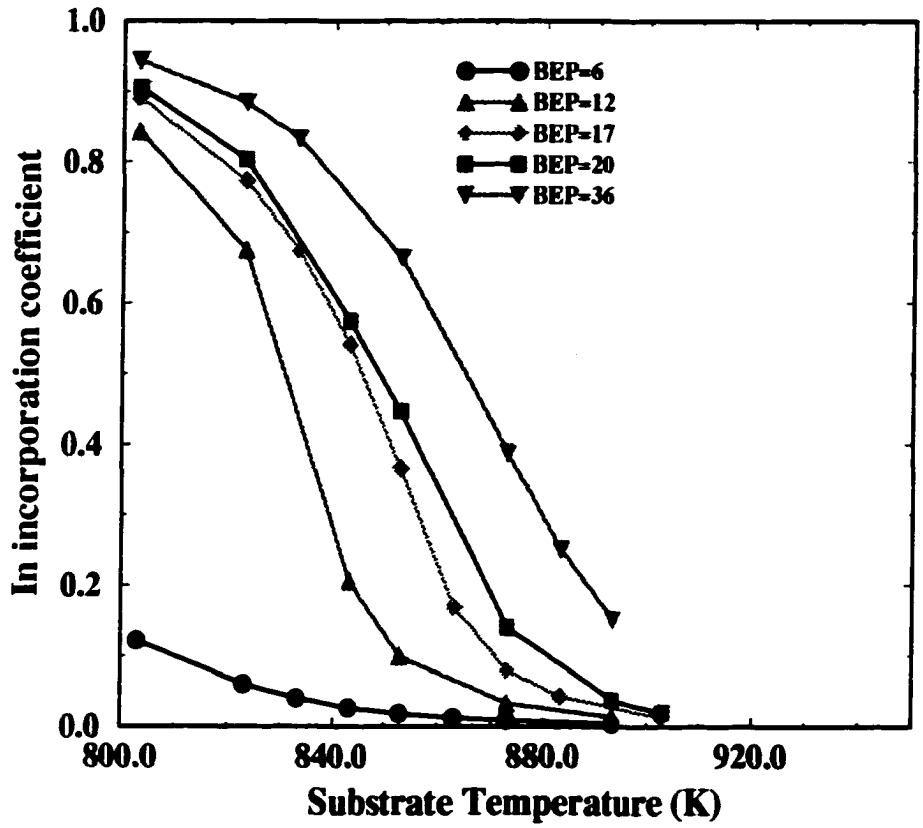

Figure 4.4: Simulation of In incorporation versus substrate temperatures for various BEPs of As_4.

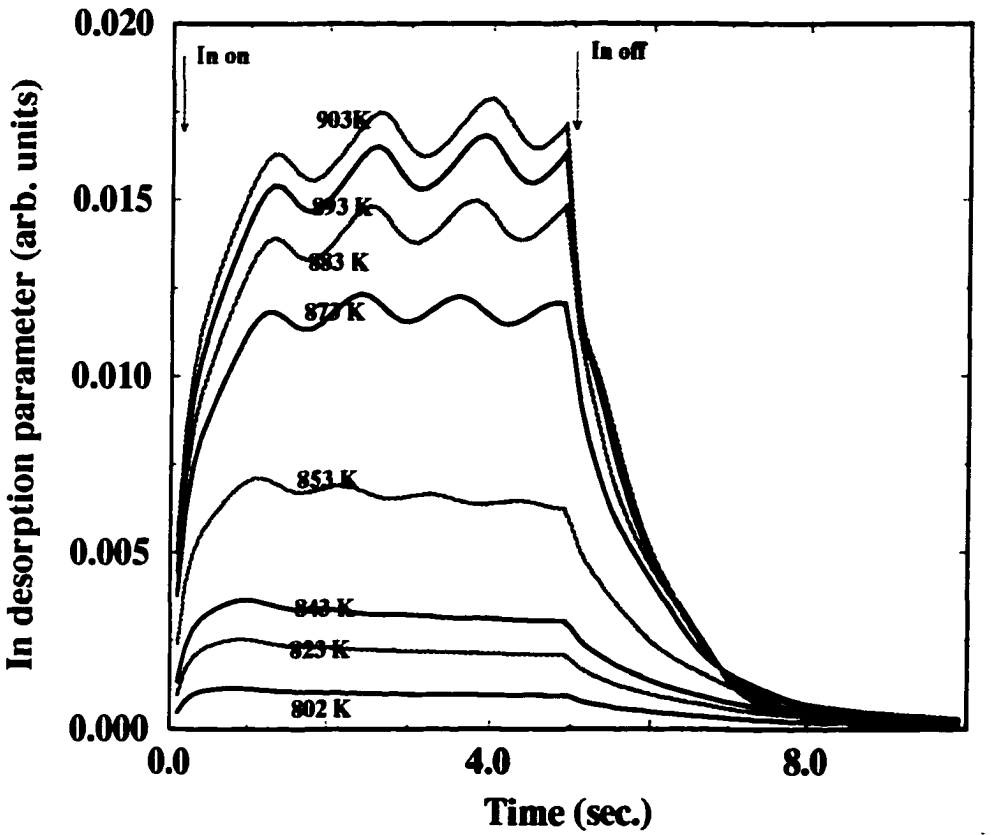

Figure 4.5: Simulation of Indium desorption rate versus time for various substrate temperatures for a As_4 BEP of 36.

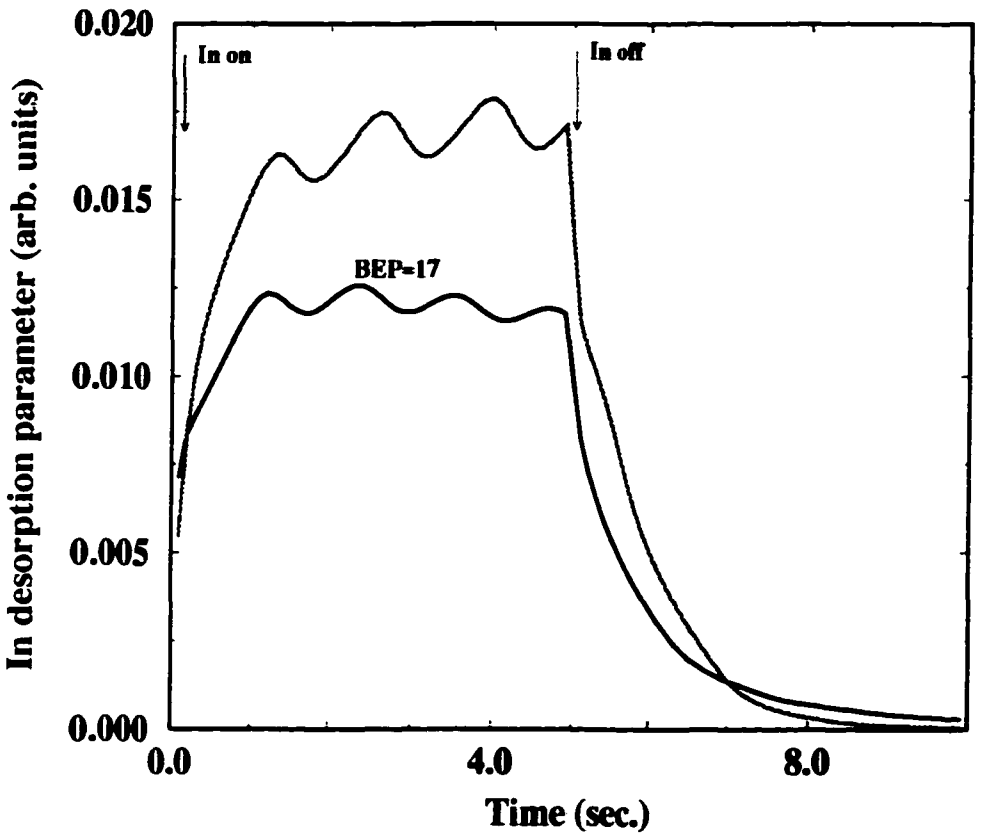

Figure 4.6: Simulation of Indium desorption rate versus time substrate temperatures 903°K for As_4 BEPs of 36 and 17.

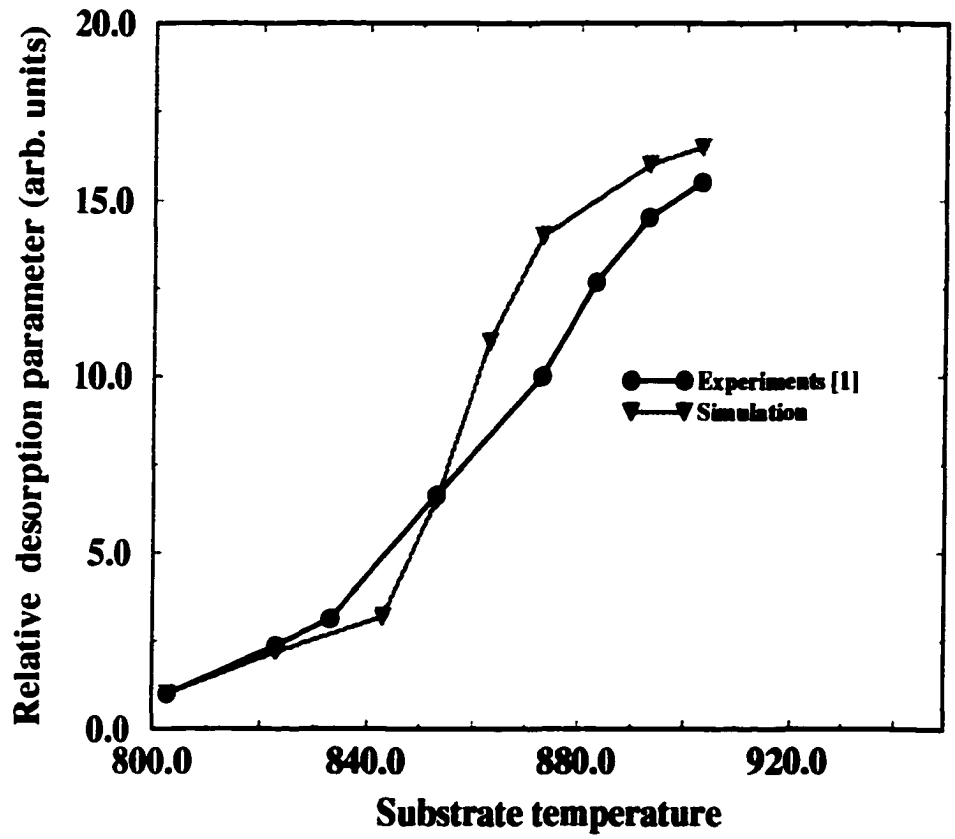

Figure 4.7: Comparison of simulation and experimental results [1] for relative desorption parameters of Indium versus substrate temperature for a As_4 BEP of 36.

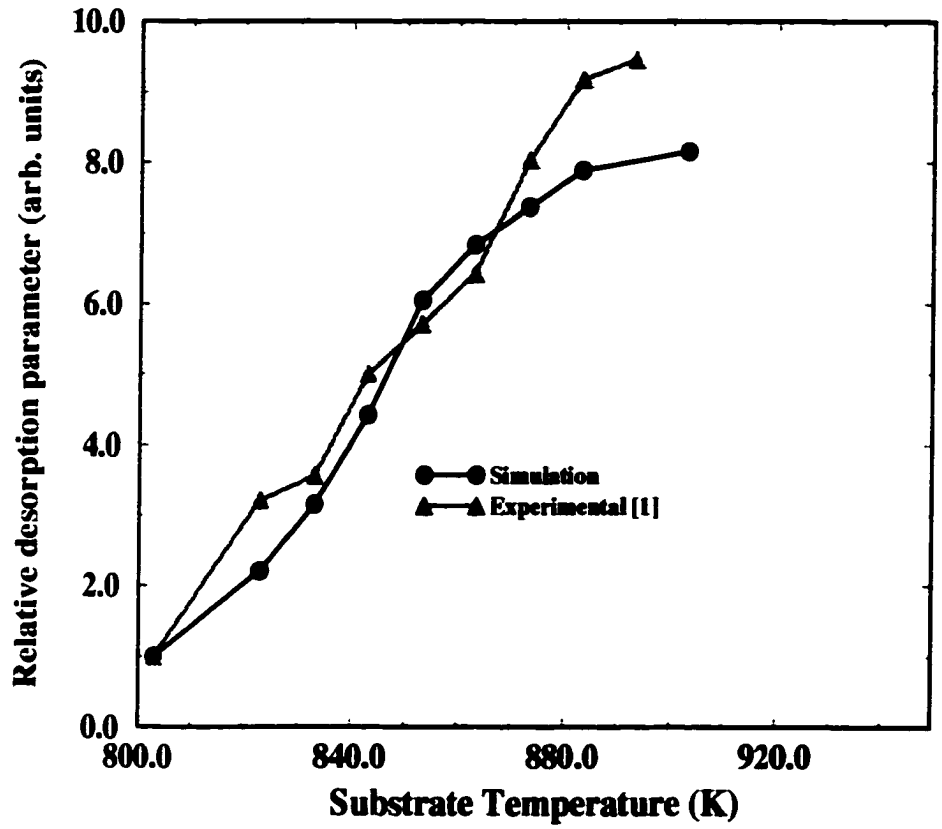

Figure 4.8: Comparison of simulation and experimental results [1] for relative desorption parameters of Indium versus substrate temperature for a As_4 BEP of 17.

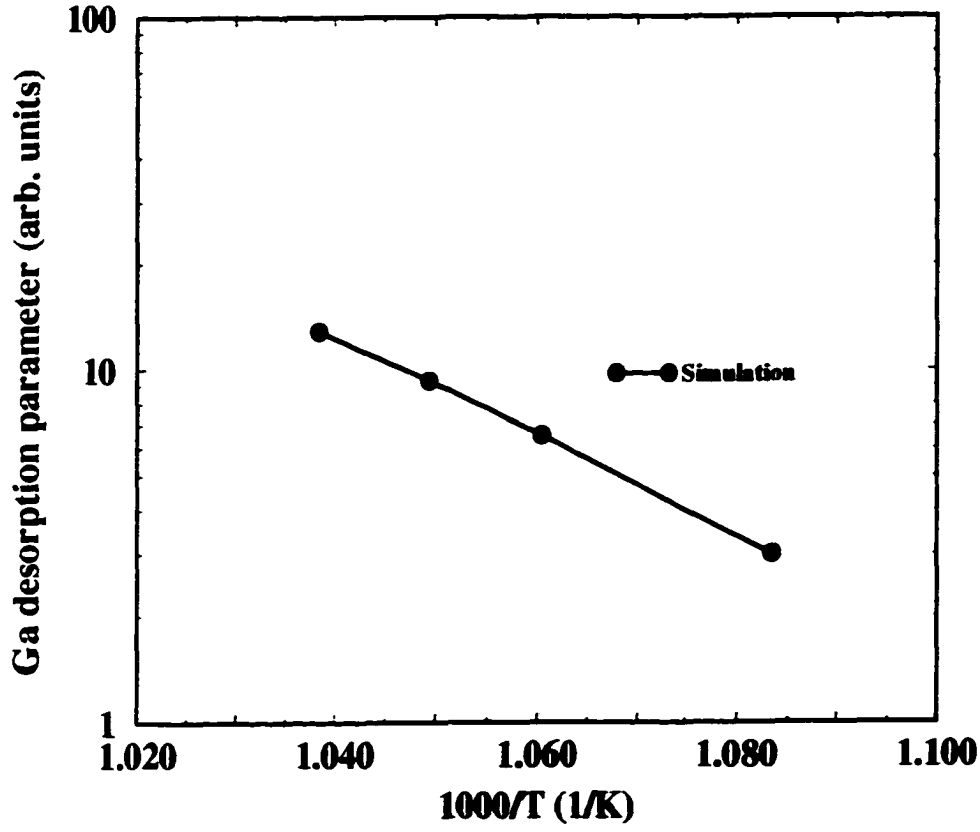

Figure 4.9: Simulation of Ga desorption rate versus inverse of substrate temperatures.

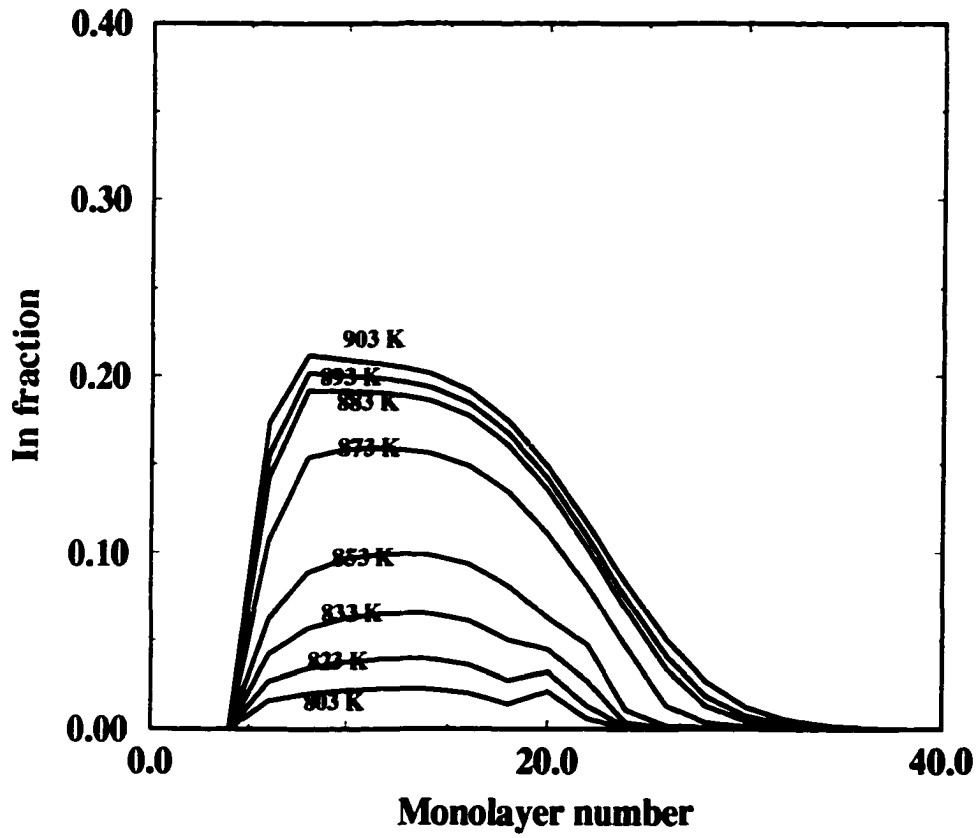

Figure 4.10: Simulation of Indium composition versus monolayer number for various substrate temperatures for a As_4 BEP of 36, for 10 sec. growth.

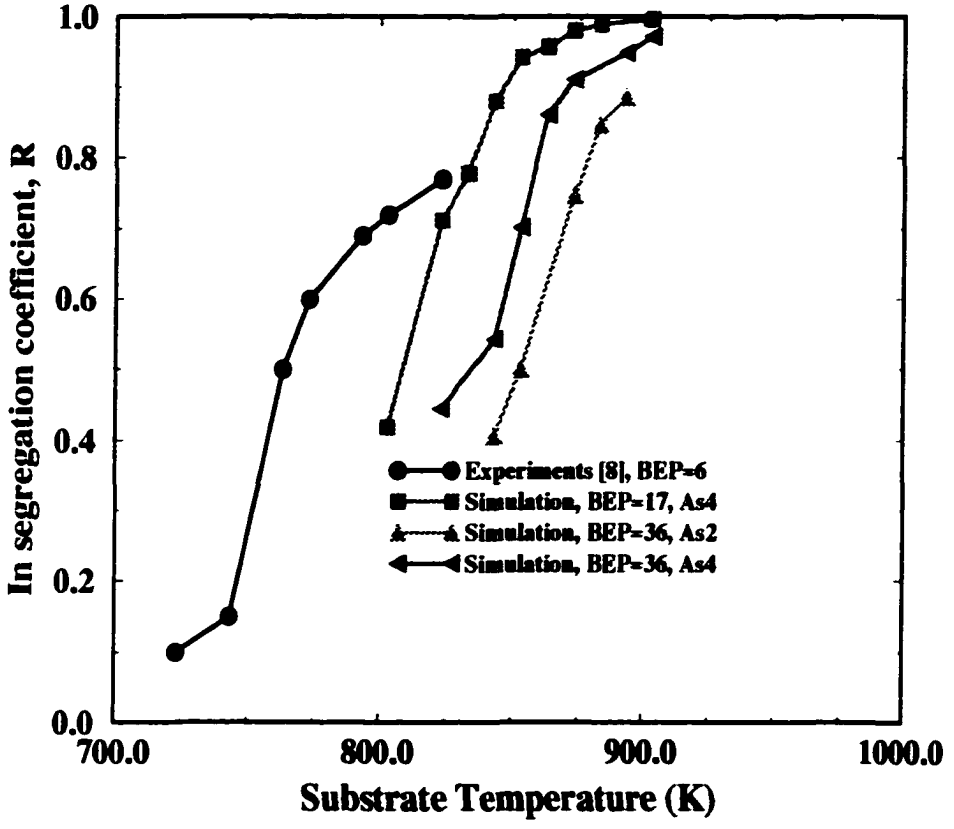

Figure 4.11: Simulation of Indium segregation versus substrate temperatures for As_4 BEPs of 36, 17 and a As_2 BEP of 36 along with the experimental data of Kao *et al* [8] for a BEP of 6.

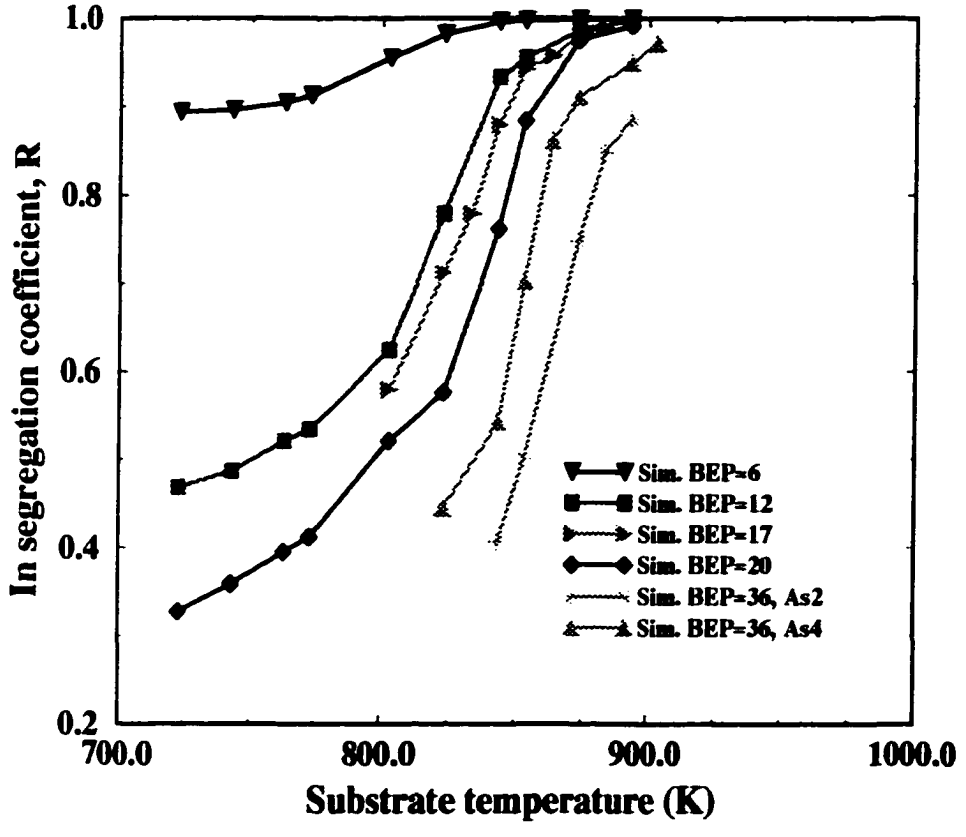

Figure 4.12: Simulation of Indium segregation versus substrate temperatures for As_4 BEPs of 36, 20, 17, 12 , and 6 and a As_2 BEP of 36.

CHAPTER 5

CONCLUSION AND RECOMMENDATIONS

5.1 Conclusion

The wide variation in the bandgap and lattice constants between $InAs$ and $GaAs$ allows for a variety of optical and electronic device applications. Many of the possible devices involve heterostructure in the active portions of the device and hence, the compositional and structural perfection of the interfaces is of paramount importance. In this materials system, the perfection is intrinsically controlled by the surface segregation of In due to its larger atomic size compared to Ga. In spite of several experimental investigations, there is a lack of a thorough understanding of the underlying surface dynamic processes and their interplay. In this work, a rate equation model is developed including several physically sound surface processes such as segregation from the crystalline layer to a surface riding In segregated layer and incorporation from the segregated In layer to crystalline layer. The rate of the processes are assumed Arrhenius type with concentration dependent activation energies. The simulated In incorporation coefficient versus substrate temperature is in excellent agreement with experimental data [1] for various As overpressure. For a constant As overpressure, In incorporation decreases with increasing temperature. For a constant temperature, In incorporation increases with increasing As overpressure. The In desorption versus time results from experiments and our simulation match very well. The desorption process has two components, one arising from the physisorbed layer of In and the other from the surface of the crystal. The activation energy for

these processes for an isolated In adatom are 0.18 eV and 2.6 eV, respectively. These observations are explained based on the interplay of competing surface processes such as segregation and incorporation.

5.2 Future Recommendations

- Simulate $GaAs$ and $InAs$ desorption versus temperatures and compare results to Zhang *et al* [3]. If results of activation energy do not agree, adjust model parameters
- Simulate pre-deposition of In to achieve abrupt $InGaAs/GaAs$ heterostructure as suggested by Kaspi *et al* [7].
- Explore independent way of obtaining bond parameters to use in the simulation instead of fitting.

BIBLIOGRAPHY

[1] Franciose Fournier and Robert. Metzler, *Growth dynamics of InGaAs/GaAs by MBE*, Journal of Crystal Growth, **175/176**, 203, (1997).

[2] K.R Evans and C. Stutz, *Incorporation and desorption rate variation at heterointerfaces in III-V MBE* , Journal of Vacuum Science and Technology,B, **9**(4), 2427, Jul/Aug (1991).

[3] J. Zhang and C. Foxon, *Modulated molecular beam study group III desorption during growth by MBE* , Journal of Crystal Growth, **111**, 93, (1991).

[4] M. Mesrine and J. Massies and M. Leroux *Indium surface segregation during chemical beam epitaxy of GaAsIn/GaAs* , Journal of Crystal Growth, **175/176**, 1242, (1997).

[5] K. Evans and C. Stutz, *Effects of strain and surface reconstruction on the kinetics of indium incorporation in MBE growth of InAs* , Journal of Crystal Growth, **95**, 197, (1989).

[6] K. Evans and R. Kaspi, *Surface chemistry evolution during MBE growth of InGaAs* , Journal of Vacuum Science and Technology,B, **13**(4), 1820, Jul/Aug (1995).

[7] R. Kaspi and K. Evans, *Improved compositional abruptness at the InGaAs on GaAs interface by presuaturation with In during MBE* , Applied Physics Letter, **67**(6), 819, August (1995).

[8] Y. Kao and F. Celli, *Detection and reduction of indium segregation during MBE growth of InGaAs/GaAs using in situ reflection mass spectroscopy*, Journal of Vacuum Science and Technology,B, **11**(3), 1023, May/Jun (1993).

[9] K. Muraki and S. Fukatsu , *Surface segregation of In atoms MBE and its influence on the levels in InGaAs/GaAs quantum wells* , Applied Physics Letter, **61**(5), 557, August (1992).

[10] Karl Woodbridge, *In incorporation in InGaAs grown by MBE*, Applied Physics Letter, **60**(23), 2911, June (1992).

[11] K. Evans and C. Stutz, *Incorporation rate variation at heterointerfaces during III-V MBE*, Applied Surface science, **56-58**, 677, (1992).

[12] G. Zhang and Ovtchinnikov, *Study growth temperature in gas-source molecular beam epitaxy growth of InGaAs/GaAs quantum well lasers* , Applied Physics Letter, **62**(9), 677, March (1993).

[13] Jean-Michael Gerard, *Growth of InGaAs/GaAs heterostructure with abrupt interfaces on the monolayer scale*, Journal of Crystal Growth, Vol.150, 1995, pp467. **150**, 467, (1995).

[14] Jean-Michael Gerard, *In situ probing at the growth temperature of the surface composition of (InGa)As and (InAl)As* , Applied Physics Letter, **61**(17), 2096, October (1993).

[15] K Radhakrishnan and S. Yoon, *Indium desorption strained InGaAs/GaAs quantum wells grown by MBE*, Journal of Vacuum Science and Technology,A, **12**(4), 1124, Jul/Aug (1994).

[16] H. Toyoshima and T. Niwa, *In surface segregation and growth-mode transition during InGaAs growth by MBE* , Applied Physics Letter, **63**(6), 8, August (1993).

[17] F. Houzay and J. Moison, *Surface segregation of third-column atoms in III-V ternary arsenide* , Journal of Crystal Growth, **95**, 35, (1989).

[18] C. Foxon and B. Joyce, *Surface processes controlling the growth of* $Ga_xIn_{1-x}As$ *by MBE*, Journal of Crystal Growth, **44**, 75, (1978).

[19] Teruo Mozume and Isao Ohbu, *Desorption of Indium during the growth of GaAs/InGaAs/GaAs Heterostructures by MBE*, Journal of Applied Physics,1992, **31**(10), 3277, (1992).

[20] D.J. Dunstan and R. Dixon, *Growth and characterization of relaxed epilayers of InGaAs on GaAs*, Journal of Crystal Growth, **126**, 589, (1993).

[21] O. M. Khreis and K. Homewood, *Interdiffusion in InGaAs/GaAs: The effect of growth conditions*, Journal of Applied Physics, **34**(1), 232, July(1998).

[22] Makoto Kudo and T. Mishima, *Highly strained InGaAs layers on GaAs grown by molecular beam epitaxy for high electron mobility transistors*, Journal of Crystal Growth, **150**, 1236, (1995).

[23] G. Price, *Growth of highly strained InGaAs on GaAs*, Applied Physics letter, **53**(14), 1288, (1988).

[24] Carrie Carter-Coman and A. Browm, *Strain-modulated epitaxy: A flexible approach to 3-D band structure* , Applied Physics letter, **69**(2), 257, (1996).

[25] T. Pinnington and C. Lavoie, *Effect of growth conditions on surface roughening of relaxed InGaAs on GaAs*, Journal of vacuum science and Technology, B, **15**(4), 1265, (1997).

[26] M. Tabuchi, *Strain energy and critical thickness of heteroepitaxial InGaAs system*, Journal of Crystal Growth, **115**, 169, (1991).

[27] s. Fujita and Y. Nakaoka, *RHEED and X-ray characterization of InGaAs/GaAs grown by MBE* , Journal of Crystal Growth, **95**, 224, (1989).

[28] C. Snyder and D. Barlett, *The MBE growth of InGaAs on GaAs(100) studied by in situ scanning tunneling microscopy and reflection high-energy electron diffraction* , Journal of vacuum science and Technology, B, **9**(4), 2189, (1991).

[29] P. Chen and T. Lee, *RHEED as a tool examining kinetic processes at MBE grown surfaces*, Growth of Compound Semiconductors, SPIE, **796**, 139, (1987).

[30] P. Ashu, J. Jefferson and A. Cullis, *Molecular Dynamics simulation of (100) InGaAs/GaAs strained-layer relaxation processes*, Journal of Crystal Growth, **150**, 176, (1995).

[31] J. Tersoff, *New empirical approach for the structure and energy of covalent systems* , Physical Review B, **37**(12), 6991, (1988).

[32] J. Tersoff, *Empirical interatomic potential for silicon with improved elastic properties* , Physical Review B, **36**(14), 9902, (1988).

[33] R. Smith *Studies in Molecular Dynamics, I. General Method,* Nucl. Instr. Methods B, **67**, 335, (1992).

[34] J. Matthews, *Accommodation of Misfit across the interface between crystals of semiconducting elements of compounds* , Journal of applied physics, **41**(9), 3800, (1970).

[35] Neave J.H., Dobson P.J., Joyce B.A., and Zhang, *Reflection high-energy diffraction oscillations from vicinal surfaces a new approach to surface diffusion measurements*, Appl. Phys. Lett. **47**, 100, (1985).

[36] Van Hove J.M., Lent C.S., Pukite P.R., and Cohen P.I, *The dependence of RHEED oscillations on MBE growth parameters* J. Vac. Sci. Technol. B, **3**, 563, (1985).

[37] A.D. Bradilsford, *Surface segregation kinetics in binary alloys*, Surf, Sci. **108**, L441 (1981).

[38] J.J. Harris, B.A. Joyce, *Adsorption-desorption studies of Ga on GaAs, Journal Crystal Growth*, **44**, 387, (1978).

[39] K. Ploog, *Molecular bean epitaxy of III-V compounds, in Crystals- Growth, Properties and Applications*, Vol.3, ed. by H. C .Freyhardt (Springer, Berlin, Heidelberg 1980) p. 73.

[40] A. Shen,*Reflection high-energy electron diffraction oscillations during growth of GaAs at low-temperature* Appl. Phys. Lett. **71**, 1540, (1997).

[41] M. Luysberg, H. Sohn, A. Prasad, P. Specht, Z. Liliental-Weber, E.R. Weber, J. Gebauer and R. Krause-Rehberg, *Effects of the growth temperature and As/Ga flux ratio on the incorporation of excess As into low-temperature grown GaAs* , J. Appl. Phys. **83**, 561, (1998).

[42] P. Specht, S. Jeong, H. Sohn, M. Luysberg, A. Prasad, J. Gebauer, R. Krause-Rehberg, E.R. Weber, *Proceedings of the Int. Conf. on Defects in Semiconductors ICDS 19, Aveiro, Portugal, Mater. Sci. Forum*, **258-263**, 951, (1997).

[43] M. Luysberg, H. Sohn, A. Prasad, P. Specht, Z. Liliental-Weber, E.R. Weber, J.Gebauer and R. Krause-Rehberg, IEEE SIMC-9., p21-26, (1996).

[44] K. Ploog, *Molecular beam epitaxy of III-V compounds, in Crystals- Growth, Properties and Applications*, **3**, ed. by H. C .Freyhardt (Springer, Berlin, Heidelberg 1980) p. 73.

[45] C.T.Foxon and B.A.Joyce, *Interaction kinetics of As_4 and Ga on (100) GaAs surfaces using MBE*, Surf. Sci. **50**, 434, 1975.

[46] A.Y. Cho and J.R. Arthur, *A study of surface reproducibility and impurity segregation of GaAs* , Prog. Solid State Chem. **10**, 157, (1975).

[47] R.C. Farrow, *Modeling of electron back scattering from topological marks low temperature*, J. Phys. D, **7**, 121, (1974).

[48] S. Muthuvenkatraman, Suresh Gorantla, Rama Venkat, Donald L. Dorsey, *A stochastic model for crystal-amorphous transition in molecular beam epitaxial Si (111)*, J. Appl. Phys.**80**, 6219, (1996).

[49] R. Venkatasubramanian, *MBE growth of compound semiconductors: part 2 stochastic modeling* , J. Mater. Res.**7**, 1221, (1992).

[50] R. Venkatasubramanian and D.L. Dorsey, *Molecular beam epitaxial growth surface roughening kinetics of Ge(001): A theoretical study*, J. Vac. Sci. and Technol. B, **11**, 253, (1993).

[51] R. Venkatasubramanian, Vamsee K. Pamula and Donald D. Dorsey, *Influence of physisorbed arsenic on RHEED intensity oscillations during low-temperature GaAs MBE*, Applied Surface Science, **104/105**, 448, (1996).

[52] S. Muthuvenkatraman, Suresh Gorantla, Rama Venkat, Donald L. Dorsey, *Antisite arsenic incorporation in the low temperature MBE of Gallium Arsenide: physics and modeling* , J. Elec. Matrls. **27/5**, 472, (1998).

[53] A.Y. Cho, *Growth of III-V semiconductors by MBE and their properties*, Thin solid films, **100**, 291, (1983).

[54] G.S. Petrich, P.R. Pukite, A.M. Wowchak, G.J. Whaley, P.L. Cohen and A.S. Arrott, *Journal of Crystal Growth*, **95**,23, (1989).

[55] R.S. Resh, K.D. Jamison, J. Strozier, A. Bensaoula and Ignatiev, *Interesting aspects of RHEED oscillations during growth of GaAs (100)*, J. Vac. Sci. Technol. B, **8**(2), 279, (1990).

[56] T. Shitara, D.D. Vvedensky, R. Wilby, J. Zhang, J.H. Neave and B.A. Joyce, *Misoreintation dependence of epitaxial growth on vicinal GaAs (001)* , Phys. Rev. B, **46**, 6825, (1992).

[57] J. Sudijono, M.D. Johnson, C.W. Snyder, M.B. Elowitz and B. Gorr, *Surface evolution during MBE desorption of GaAs*, Phys. Rev. Lett. **69**, 2811, (1992).

[58] A.M. Dabiran, P.I. Cohen, J.E. Angelo and W.W. Gerberich, *RHEED measurements of molecular beam epitaxy grown GaAs and InGaAs on GaAs (111)*, Thin solid films, **231**, 1-7, (1993).

[59] A. Madhukar and S.V. Ghaisas, *Implications of the configuration-dependent reactive incorporation process for the group V pressure* , Appl. Phys. Lett. **47**, 3, (1985).

[60] F. H. Stillinger, T.A. Weber, *Computer simulation of local order in condensed phases of silicon*, Phys. Rev. B, **31**, 5262, (1985).

[61] B.W. Dodson and P.A. Taylor, *Molecular dynamics simulation of the growth of strained-layer lattices*, Phys. Rev. B, **36**, 1355, (1987).

[62] M. Schneider, I.K. Schuller and A. Rahman, *Epitaxial growth of silicon: A molecular-dynamics simulation*, Phys. Rev. B, **36**, 1340, (1987).

[63] Shridhar Bendi, R. Venkatasubramanian, D.L. Dorsey, *Molecular beam epitaxy doping kinetics: A rate equation model*, J. Appl. Phys. **76**,(9), 5202, (1994).

[64] T.B. Joyce and T.J. Bullough *Effect of growth conditions on surface relaxation during MBE*, Journal of Crystal Growth, **127**, 265, (1993).

[65] J. F. Walker and J. Bonar *SPIE, Growth of Semiconductor Structures*,**1285**, 122 (1990).

[66] M. A. Herman and H. Sitter *Molecular Beam Epitaxy*, 1996.

[67] Jeffrey Y. Tsao, *Materials Fundamentals of Molecular Beam Epitaxy*, 1993.

[68] J. Nicolas, *Computational Physics*, 1997.

[69] An-Ban Chen and A Sher, *Semiconductor Alloys*, 1995.

[70] K. Natarajan, R. Venkatasubramanian, D.L. Dorsey, *Low-temperature molecular beam epitaxy of GaAs: A theoretical study*, J. Vac. Sci. Technol. B, **17**,(3), 1227, (1999).

VITA

Graduate College
University of Nevada, Las Vegas

Golshan Colayni

Local Address:
4236 Claymont Street #1
Las Vegas, NV 89119

Degrees:
Bachelor of Science, Physics, 1991
Sharif University and Technology, Tehran, Iran

Master of Science, Physics, 1993
Azad University, Tehran, Iran

Thesis Title:Theoretical studies of Molecular Beam Epitaxy Growth of InGaAs semiconductor compound on Gallium Arsenide Substrate

Thesis Examination Committee:
Chairperson, Dr. Rama Venkat, Ph.D.
Committee Member, Dr. Shahram Latifi, Ph.D.
Committee Member, Dr. Rahim Khoie Ph.D.
Graduate Faculty Representative, Dr. Chengfeng Chen, Ph.D.